RESEARCH ARTICLE

A Nonlinear Dynamical Model of Divorce Due to Extra-Marital Affairs with Long-Distance and Age-Structured Influences

Sarita Pippal[1,*] **and Ajay Ranga**[2]

[1] Department of Mathematics, Panjab University, Chandigarh, India
[2] J.C. Bose University of Sciences and Technology, YMCA, Faridabad, India

Abstract

This study introduces an age-structured compartmental model that analyzes transitions among stable marriages, long-distance relationships, extra-marital affairs, and divorce. Key behavioral parameters include λ (transition to long-distance), δ (reunification), α_1 and α_2 (affair formation), β (reconciliation), γ (affair-driven divorce), and μ (non-affair divorce). The unmarried women's pool is structured by age, governed by an engagement function $\theta(a)$ and inflow $\Lambda(a)$. A nonlinear differential equation system captures how behavioral mechanisms collectively drive marital dynamics over time. Numerical simulations show that higher β and δ enhance stability through reconciliation and reunification, while increases in λ, α_1, and α_2 raise affair prevalence and divorce. Larger γ and μ further destabilize marriages, increasing the unmarried population. Bifurcation-style plots reveal the nonlinear interplay among parameters and their influence on equilibrium states. The system admits two meaningful equilibria: an age-only state and an interior coexistence state. Stability is determined by a cubic characteristic polynomial; Routh–Hurwitz conditions yield explicit threshold inequalities. Stability persists when dissolution and extramarital transition rates are low, whereas exceeding these thresholds leads to demographic imbalance or oscillations. Overall, the findings underscore the balance between individual behavior and societal intervention. Strengthening social support and reducing separation incentives are suggested strategies to promote marital stability and reduce divorce prevalence.

Keywords: mathematical modeling, marital dynamics, social contagion, nonlinear systems.

1 Introduction

Marriage is a universally recognized social institution that forms the foundation of family life and plays a central role in maintaining the structure and stability of societies [1]. However, in recent decades, divorce has become an increasingly common phenomenon globally, affecting individuals across diverse cultures, religions, and socioeconomic statuses. Divorce has emerged as a critical social issue across the globe, with increasing rates observed in both developed

Submitted: 26 October 2025
Accepted: 24 November 2025
Published: 10 December 2025

Vol. 1, **No.** 2, 2025.
10.62762/JNDA.2025.544526

***Corresponding author:**
✉Sarita Pippal
saritamath@pu.ac.in

Citation
Pippal, S., & Ranga, A. (2025). A Nonlinear Dynamical Model of Divorce Due to Extra-Marital Affairs with Long-Distance and Age-Structured Influences. *Journal of Nonlinear Dynamics and Applications*, 1(2), 76–98.

and developing nations. It not only affects the individuals directly involved but also has widespread consequences on children, families, and broader society. Factors such as changing cultural norms, economic stress, diminished social support, and evolving expectations from marriage contribute to the rising trend. Divorce often leads to psychological distress, financial instability, and disruptions in children's well-being and education. From a demographic and policy perspective, understanding the drivers of divorce is essential for designing effective interventions to promote stable family structures and support marital relationships. Mathematical modeling provides a valuable tool to systematically analyze the complex interplay of behavioral, emotional, and social variables influencing divorce, offering evidence-based insights for social planning and reform. Studies have shown that divorce rates are rising in various countries such as the United States, England, Wales, Spain, and several African nations [1–4]. In particular, sub-Saharan Africa has witnessed a sharp increase in divorce cases among younger couples [5].

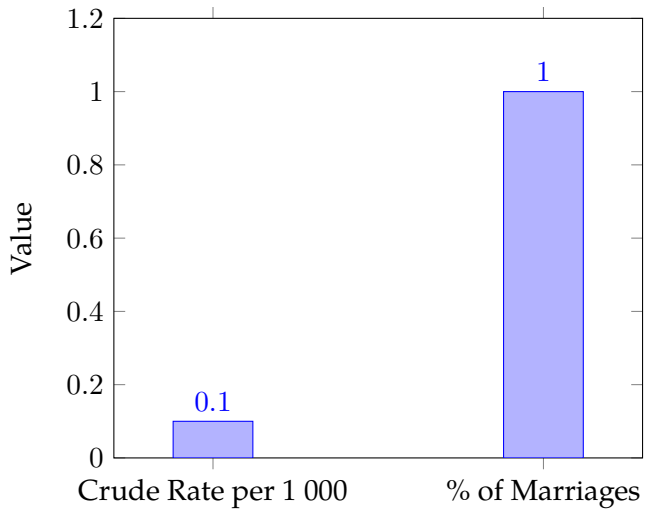

Figure 1. India's divorce indicators: crude divorce rate at approximately 0.1 divorces per 1000 people (2021) and about 1% of marriages end in divorce.

Figure 1 illustrates two key divorce-related indicators in the Indian context. The first bar shows the crude divorce rate, which remains remarkably low at approximately 0.1 divorces per 1,000 individuals as of 2021. The second bar highlights that only about 1% of marriages in India end in divorce. These values reflect the cultural, social, and institutional factors that contribute to marital stability in India, despite increasing modernization and shifts in family norms. Compared to global trends, India's divorce rates remain among the lowest, underscoring the enduring influence of traditional marital values and societal expectations. Divorce can result from a wide range of personal, social, and economic factors. Commonly cited reasons include lack of compatibility, emotional or physical abuse, infidelity, unmet expectations, and communication breakdowns. In the Indian context, additional contributors may include pressure from extended families, dowry-related disputes, infertility, and rigid gender roles. With increasing urbanization, education, and financial independence—especially among women—there is a growing assertion of individual autonomy, which can sometimes challenge traditional marital structures. Moreover, changing societal attitudes have gradually reduced the stigma around divorce, leading more individuals to seek legal separation when faced with persistent marital conflict or dissatisfaction. While some divorces stem from irreconcilable differences, others are driven by the pursuit of mental well-being and dignity.

Divorce has profound psychological, social, and economic impacts on individuals and society [6, 7]. Extramarital affairs and long-distance relationships have emerged as significant contributors to marital breakdown in modern society. Extramarital affairs often result in a breach of trust, emotional disconnect, and irreparable damage to the marital bond, making reconciliation difficult. Long-distance relationships, on the other hand, introduce physical separation, communication gaps, and emotional strain, which can weaken the stability of a marriage over time. When these factors are left unaddressed, they can lead to increased dissatisfaction, detachment, and ultimately, divorce. Incorporating these elements into mathematical modeling offers valuable insight into how interpersonal and spatial dynamics influence the overall trajectory of marital outcomes. The increasing prevalence of divorce has stimulated mathematical modeling efforts aimed at understanding its dynamics from a social contagion perspective, drawing inspiration from infectious disease models.

- **Classical Compartmental Models** Early mathematical frameworks for marriage and divorce often use compartmental approaches inspired by epidemiology, such as the Married–Separated–Divorced (MSD) models. These models categorize populations into mutually exclusive marital states and govern transitions between them with marriage, separation, reconciliation, and divorce rates [1, 2]. Such models provide foundational insights into the spread and containment of divorce as a social

phenomenon.

- **Fuzzy Logic and Uncertainty Models** To capture human behavioral uncertainty, fuzzy logic has been incorporated in Single–Married–Broken–Divorced (SMBD) models. These models allow gradual membership values to account for partial reconciliation or marital instability, reflecting the complexity and non-binary nature of marital states. Sensitivity analysis in these studies identifies key parameters influencing divorce dynamics, supporting targeted social interventions.
- **Social Contagion and Network-Based Approaches** Recent work models divorce as a social contagion spreading across social networks [3, 8]. These approaches use epidemiological metrics like a reproduction number to characterize conditions for divorce amplification or mitigation. Factors such as peer influence, conflict rates, and reconciliation probabilities emerge as crucial determinants of marital stability.

1.1 Model Extensions Incorporating Affairs and Distance

Most existing models primarily focus on direct marital states such as stable, separated, or divorced categories. However, extramarital affairs and long-distance relationships play significant roles in marital breakdown, yet are underrepresented in mathematical studies [4, 5]. Incorporating these elements better captures the complex interpersonal and spatial factors influencing divorce.

This study advances the literature by developing an age-structured compartmental model that explicitly includes unmarried women and models transitions involving extramarital affairs and long-distance marriages within a nonlinear, saturating framework. The model leverages age-dependent engagement probabilities and multi-parameter bifurcation analyses to reveal the intricate interactions between behavioral and demographic factors shaping the dynamics of marriage and divorce. Inspired by infectious disease modeling, we classify the population into compartments representing stable marriages, long-distance couples, affair-involved couples, and divorced individuals. Transition rates reflect behavioral tendencies such as dissatisfaction, physical separation, and social reinforcement. Through numerical simulations across varying parameter sets, the model captures nonlinear effects that determine conditions for marital stability or breakdown. This framework contributes to the growing body of work applying mathematical tools to social phenomena, providing quantitative insight into how infidelity and geographic separation affect marital outcomes.

2 Marriage–Affair–Divorce Model with Age-Structured Unmarried Women

Let the total married population at time t be classified into the following compartments:

- $M(t)$: Stable married couples,
- $L(t)$: Long-distance or absentee married couples,
- $A(t)$: Couples involved in extra-marital affairs,
- $D(t)$: Divorced couples,
- $U_a(t)$: Unmarried women of age $a \in [a_{\min}, a_{\max}]$ involved with married men.

The total married population is given by

$$N = M(t) + L(t) + A(t) + D(t).$$

The model parameters are summarized in Table 1.

2.1 Age Influence Function

The age-dependent probability density of unmarried women engaging in affairs is modeled by a normalized Gaussian function:

$$\theta(a) = \frac{1}{\sqrt{2\pi\sigma^2}} \exp\left(-\frac{(a-a_0)^2}{2\sigma^2}\right),$$

where a_0 represents the most active age (e.g., 25 years), and σ is the spread parameter.

2.2 Model Equations

The dynamics of the system are described by the following nonlinear differential equations:

Table 1. Model parameters and their descriptions.

Parameter	Description
λ	Transition rate from stable to long-distance marriages
δ	Reunification rate from long-distance to stable marriages
α_1	Affair formation rate from stable marriages
α_2	Affair formation rate from long-distance marriages
β	Reconciliation rate from affair back to stable marriage
γ	Divorce rate due to affairs
μ	Divorce rate from stable marriages unrelated to affairs
K	Carrying capacity (saturation level) of affairs
$\theta(a)$	Probability density of unmarried women of age a engaging in affairs
$\Lambda(a)$	Inflow of new unmarried women into age class a
$\mu_u(a)$	Exit or aging rate from the unmarried pool at age a

$$\frac{dM}{dt} = -\lambda M - \alpha_1 M\left(1-\frac{A}{K}\right) + \delta L + \beta A - \int_{a_{\min}}^{a_{\max}} \theta(a) U_a M \, da, \tag{1}$$

$$\frac{dL}{dt} = \lambda M - \delta L - \alpha_2 L\left(1-\frac{A}{K}\right), \tag{2}$$

$$\frac{dA}{dt} = \alpha_1 M\left(1-\frac{A}{K}\right) + \alpha_2 L\left(1-\frac{A}{K}\right) + \int_{a_{\min}}^{a_{\max}} \theta(a) U_a M \, da - (\beta+\gamma)A, \tag{3}$$

$$\frac{dD}{dt} = \gamma A + \mu M, \tag{4}$$

$$\frac{dU_a}{dt} = \Lambda(a) - \theta(a) U_a M - \mu_u(a) U_a. \tag{5}$$

2.3 Model Interpretation

- The terms $\alpha_1 M(1 - A/K)$ and $\alpha_2 L(1 - A/K)$ capture bounded (logistic-type) affair formation. The saturation effect represents the limited social or emotional capacity for new affairs as A approaches K.
- The integral term $\int_{a_{\min}}^{a_{\max}} \theta(a) U_a M \, da$ accounts for interactions between married men and unmarried women across age groups.
- The U_a compartment captures demographic processes: inflow of new unmarried women ($\Lambda(a)$), depletion due to coupling with married men, and natural exit or aging ($\mu_u(a)U_a$).

3 Theoretical Framework and Relation to Infectious Disease Modeling

The mathematical structure of the proposed marriage–affair–divorce model draws conceptual parallels with classical infectious disease frameworks, particularly Susceptible–Infected–Recovered (SIR) models. In epidemiology, individuals transition between disease compartments based on transmission, recovery, and mortality rates. Analogously, in this socio-behavioral context, couples transition among distinct marital states—stable, long-distance, affair-involved, and divorced—through behavioral and psychosocial interactions.

From a theoretical standpoint, the model exhibits several features analogous to infection dynamics:

- The compartment of stable marriages $M(t)$ resembles the susceptible class, which may transition into the "affair" or "infection" state via contact-induced processes represented by α_1, α_2, and $\theta(a)$.
- Affair formation acts as the transmission mechanism, governed by logistic saturation $\left(1 - \frac{A}{K}\right)$ and modulated by social exposure intensity.
- The reconciliation process (β) corresponds to recovery phenomena, returning affected couples back to a stable state.
- Divorce processes (γ and μ) represent permanent removals from the active marital pool, analogous to disease-induced or natural removal in infection models.
- The integral term $\int_{a_{\min}}^{a_{\max}} \theta(a) U_a M \, da$ plays a role similar to an age-dependent force of infection, weighted by a partner interaction kernel $\theta(a)$.

These analogies allow analytical tools developed in infectious disease theory to be extended to marital dynamics, including threshold conditions and

equilibrium stability. In particular, a reproductive threshold quantity can be defined to describe the expected number of new affair formations produced by one existing affair case in an otherwise stable population. Denoting this as a social reproduction number, R_s, it provides a threshold criterion separating marital stability ($R_s < 1$) from instability and widespread extra-marital engagements ($R_s > 1$).

Future theoretical extensions may employ next-generation matrix methods to compute R_s and analyze local and global stability of equilibrium points. Such theoretical insights strengthen the socio-mathematical interpretation of the model, bridging behavioral social processes with established epidemiological modeling frameworks.

These transitions between marital states are visually summarized in the compartmental diagram shown in Figure 2.

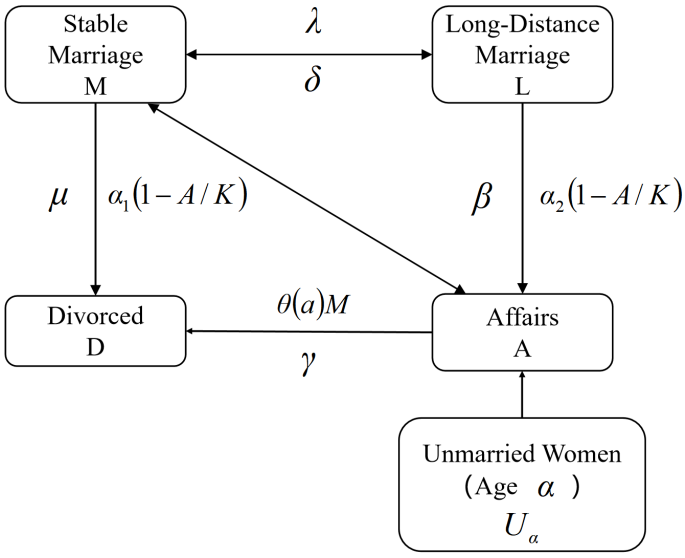

Figure 2. State transition diagram illustrating marriage dynamics with extra-marital affairs, divorce, and age-structured unmarried women.

4 Preliminaries

Definition 4.1 (Autonomous and Non-autonomous Systems). *Consider the general dynamical system*

$$\dot{\mathbf{X}} = \mathbf{F}(\mathbf{X}, t), \qquad \mathbf{X}(t) \in \mathbb{R}^n, \tag{6}$$

where $\mathbf{F} : \mathbb{R}^n \times \mathbb{R} \to \mathbb{R}^n$ *is sufficiently smooth.*

- *The system is called* non-autonomous *if* $\mathbf{F}$ *depends on* t *explicitly.*
- *If* $\mathbf{F}$ *depends only on the state vector* $\mathbf{X}$*, then*

$$\dot{\mathbf{X}} = \mathbf{F}(\mathbf{X})$$

defines an autonomous *system.*

The marital–dynamics model considered throughout this work is autonomous because the right-hand side depends solely on the system states.

Definition 4.2 (Trajectory (Orbit)). *Given an initial condition* $\mathbf{X}(t_0) = \mathbf{X}_0$*, the associated solution* $\mathbf{X}(t) = \varphi(t; t_0, \mathbf{X}_0)$ *is called the* trajectory *or* orbit *through* $\mathbf{X}_0$*. The collection of points traced by the solution is*

$$\gamma(\mathbf{X}_0) = \{\varphi(t; t_0, \mathbf{X}_0) : t \geq t_0\}.$$

Definition 4.3 (Invariant Set). *A subset* $S \subseteq \mathbb{R}^n$ *is said to be* invariant *for system* (6) *if for every* $\mathbf{X}_0 \in S$*, the corresponding trajectory satisfies* $\varphi(t; t_0, \mathbf{X}_0) \in S$ *for all* $t \geq t_0$*.*

Definition 4.4 (Equilibrium Point). *A point* $\mathbf{X}^* \in \mathbb{R}^n$ *is an* equilibrium *of* (6) *if it satisfies*

$$\mathbf{F}(\mathbf{X}^*) = \mathbf{0}.$$

Lemma 4.5 (Linear Stability of Autonomous Systems). *Let*

$$\dot{\mathbf{X}} = \mathbf{F}(\mathbf{X}),$$

where $\mathbf{F}$ *is continuously differentiable on an open set* $D \subset \mathbb{R}^n$*, and let* $\mathbf{X}^* \in D$ *be an equilibrium. The stability of* $\mathbf{X}^*$ *is determined by the Jacobian*

$$J(\mathbf{X}^*) = D\mathbf{F}(\mathbf{X}^*).$$

- *If all eigenvalues of* $J(\mathbf{X}^*)$ *have strictly negative real parts, then* $\mathbf{X}^*$ *is* locally asymptotically stable.
- *If at least one eigenvalue has a positive real part,* $\mathbf{X}^*$ *is* unstable.
- *If one or more eigenvalues have zero real part, the Jacobian test is inconclusive and nonlinear techniques (e.g., center manifold theory) must be used.*

Lemma 4.6 (Classification of Equilibria in the Marital Dynamics Model). *For the system with state vector* $\mathbf{X}(t) = (M(t), L(t), A(t), D(t), U_a(t))^\top$*, two main classes of equilibria arise:*

1. Trivial (marriage-free) equilibrium: *characterized by vanishing marital compartments.*
2. Non-trivial (coexistence) equilibrium: *where all compartments maintain strictly positive steady-state values.*

Definition 4.7 (Jacobian Matrix). *For a vector field* $\mathbf{F} = (F_1, \ldots, F_n)^\top$*, the Jacobian evaluated at* $\mathbf{X}$ *is given by*

$$J(\mathbf{X}) = \left[\frac{\partial F_i}{\partial X_j}(\mathbf{X})\right]_{i,j=1}^{n},$$

and provides the local linear approximation of the dynamics near $\mathbf{X}$*.*

Definition 4.8 (Stability of an Equilibrium). *An equilibrium* $\mathbf{X}^*$ *is*

- locally stable *if all trajectories that start sufficiently close remain close,*
- locally asymptotically stable *if it is stable and* $\varphi(t; t_0, \mathbf{X}_0) \to \mathbf{X}^*$ *as* $t \to \infty$*,*
- unstable *if trajectories starting arbitrarily near can diverge away.*

Definition 4.9 (Hyperbolic Equilibrium). *An equilibrium* $\mathbf{X}^*$ *is* hyperbolic *when the Jacobian* $J(\mathbf{X}^*)$ *has no eigenvalues on the imaginary axis. Such equilibria inherit the stability dictated by the signs of the real parts of their eigenvalues.*

Lemma 4.10 (Routh–Hurwitz Criterion for Cubic Polynomials). *For the cubic polynomial*

$$\lambda^3 + c_1\lambda^2 + c_2\lambda + c_3 = 0,$$

all roots have negative real parts if and only if

$$c_1 > 0, \qquad c_2 > 0, \qquad c_3 > 0, \qquad c_1c_2 > c_3.$$

Definition 4.11 (Basic Reproduction Number). *The* basic reproduction number $\mathcal{R}_0$ *is a key threshold indicator describing the expected number of new transitions generated by a single individual introduced into an otherwise fully receptive population* [9–11].

Interpretation:

- $\mathcal{R}_0 < 1$*: the undesirable state eventually disappears,*
- $\mathcal{R}_0 > 1$*: the undesirable state persists,*
- $\mathcal{R}_0 = 1$*: the system lies at a threshold, often associated with bifurcation.*

Next-Generation Matrix Approach. *For systems of the form*

$$\dot{\mathbf{X}} = \mathbf{F}(\mathbf{X}) - \mathbf{V}(\mathbf{X}),$$

where $\mathbf{F}$ *contains the new-introduction terms and* $\mathbf{V}$ *collects all other transitions, the process is:*

1. *identify the "infected" or target compartments,*
2. *evaluate the Jacobians*

$$F = \left.\frac{\partial \mathbf{F}}{\partial \mathbf{X}}\right|_{CFE}, \qquad V = \left.\frac{\partial \mathbf{V}}{\partial \mathbf{X}}\right|_{CFE},$$

3. *form the next-generation matrix* $K = FV^{-1}$*,*
4. *compute the spectral radius* $\mathcal{R}_0 = \rho(K)$*.*

This framework, commonly used in epidemiology, applies equally to social dynamics such as marital or crime propagation models.

5 Qualitative Analysis of the present Model

Theorem 5.1 (Positivity of Solutions). *Suppose the initial data satisfy*

$$\begin{aligned} &M(0) \geq 0, \quad L(0) \geq 0, \quad A(0) \geq 0, \\ &D(0) \geq 0, \quad U_a(0) \geq 0, \quad \forall\, a \in [a_{\min}, a_{\max}], \end{aligned} \tag{7}$$

and all parameters and coefficient functions are non-negative:

$$\lambda,\ \delta,\ \alpha_1,\ \alpha_2,\ \beta,\ \gamma,\ \mu,\ K,\ \theta(a),\ \Lambda(a),\ \mu_u(a)\ \geq 0. \tag{8}$$

Then every solution of system (1)–(5) *remains non-negative for all* $t \geq 0$*.*

Proof. We verify positivity for each component using the integrating factor method.

1. Positivity of $M(t)$

The equation for M may be written as

$$\frac{dM}{dt} + \left[\lambda + \alpha_1\left(1 - \frac{A}{K}\right) + \int_{a_{\min}}^{a_{\max}} \theta(a)U_a\, da\right] M = \delta L + \beta A. \tag{9}$$

Define

$$p_M(t) := \lambda + \alpha_1\left(1 - \frac{A}{K}\right) + \int_{a_{\min}}^{a_{\max}} \theta(a)U_a\, da\ \geq 0, \tag{10}$$

$$q_M(t) := \delta L + \beta A\ \geq 0. \tag{11}$$

Multiplying (9) by the integrating factor

$$\mu_M(t) = \exp\left(\int_0^t p_M(s)\, ds\right) > 0, \tag{12}$$

gives

$$\frac{d}{dt}(M\,\mu_M) = q_M(t)\,\mu_M(t) \geq 0.$$

Integrating from 0 to t,

$$M(t) = \frac{M(0) + \displaystyle\int_0^t q_M(s)\,\mu_M(s)\, ds}{\mu_M(t)}\ \geq 0. \tag{13}$$

2. Positivity of $L(t)$

Rewrite the L-equation as

$$\frac{dL}{dt} + \left[\delta + \alpha_2\left(1 - \frac{A}{K}\right)\right] L = \lambda M. \tag{14}$$

Let

$$p_L(t) := \delta + \alpha_2\left(1 - \frac{A}{K}\right) \geq 0, \tag{15}$$

$$q_L(t) := \lambda M \geq 0. \tag{16}$$

With integrating factor

$$\mu_L(t) = \exp\left(\int_0^t p_L(s)\, ds\right), \tag{17}$$

the solution is

$$L(t) = \frac{L(0) + \int_0^t q_L(s)\, \mu_L(s)\, ds}{\mu_L(t)} \geq 0. \tag{18}$$

3. Positivity of $A(t)$

The equation for A is

$$\begin{aligned}\frac{dA}{dt} + (\beta + \gamma)A &= \alpha_1 M\left(1 - \frac{A}{K}\right) \\ &\quad + \alpha_2 L\left(1 - \frac{A}{K}\right) + M\int_{a_{\min}}^{a_{\max}} \theta(a) U_a\, da.\end{aligned} \tag{19}$$

Since the right-hand side is non-negative, define

$$\begin{aligned}p_A(t) &:= \beta + \gamma, \\ q_A(t) &:= \alpha_1 M\left(1 - \frac{A}{K}\right) + \alpha_2 L\left(1 - \frac{A}{K}\right) \\ &\quad + M\int \theta(a) U_a\, da \ \geq 0.\end{aligned} \tag{20}$$

Following the same integrating-factor argument used for M and L, we obtain

$$A(t) \geq 0, \qquad t \geq 0. \tag{21}$$

4. Positivity of $D(t)$

The equation

$$\frac{dD}{dt} = \gamma A + \mu M \geq 0 \tag{22}$$

shows that $D(t)$ is non-decreasing. Hence, with $D(0) \geq 0$,

$$D(t) \geq 0, \qquad t \geq 0. \tag{23}$$

5. Positivity of $U_a(t)$

For each fixed $a \in [a_{\min}, a_{\max}]$,

$$\frac{dU_a}{dt} + [\theta(a)M + \mu_u(a)]\, U_a = \Lambda(a) \geq 0. \tag{24}$$

Using integrating factor

$$\mu_{U_a}(t) = \exp\left(\int_0^t [\theta(a)M(s) + \mu_u(a)]\, ds\right), \tag{25}$$

gives

$$U_a(t) = \frac{U_a(0) + \int_0^t \Lambda(a)\, \mu_{U_a}(s)\, ds}{\mu_{U_a}(t)} \geq 0. \tag{26}$$

Since all components remain non-negative for all $t \geq 0$, the theorem is proved. □

Theorem 5.2 (Boundedness of All State Variables)**.** *Assume that the total population*

$$N(t) = M(t) + L(t) + A(t) + D(t) \tag{27}$$

satisfies the uniform bound

$$0 \leq N(t) \leq N_{\max}, \qquad \forall t \geq 0. \tag{28}$$

Let the age–dependent functions obey

$$\Lambda(a) > 0, \qquad \mu_u(a) > 0, \qquad \forall a \in [a_{\min}, a_{\max}]. \tag{29}$$

Then all demographic compartments satisfy

$$0 \leq M(t), L(t), A(t), D(t) \leq N_{\max}, \tag{30}$$

and the age–structured class satisfies

$$0 \leq U_a(t) \leq \frac{\Lambda(a)}{\mu_u(a)}, \qquad \forall t \geq 0. \tag{31}$$

Thus the solution remains in a compact, positively invariant region.

Proof. The proof proceeds in several structured steps.

- **Step 1:**

  Boundedness of the demographic compartments.

  From (27), each component is a subpopulation of the total; hence,

  $$0 \leq M(t), L(t), A(t), D(t) \leq N(t).$$

  Using the global in-time bound (28) yields

  $$0 \leq M(t), L(t), A(t), D(t) \leq N_{\max}, \qquad \forall t \geq 0. \tag{32}$$

- **Step 2:**

  Differential inequality for the age–structured variable.

  Consider

$$\frac{dU_a}{dt} = \Lambda(a) - \theta(a)M(t)U_a(t) - \mu_u(a)U_a(t). \quad (33)$$

  Since the nonlinear term is nonpositive,

$$-\theta(a)M(t)U_a(t) \le 0,$$

  we obtain the comparison inequality

$$\frac{dU_a}{dt} \le \Lambda(a) - \mu_u(a)U_a(t). \quad (34)$$

- **Step 3:**

  Solution of the associated linear problem.

  Consider the auxiliary equation

$$\frac{dZ}{dt} = \Lambda(a) - \mu_u(a)Z(t). \quad (35)$$

  Solving (35) via integrating factor gives

$$Z(t) = \frac{\Lambda(a)}{\mu_u(a)} + \left(Z(0) - \frac{\Lambda(a)}{\mu_u(a)}\right)e^{-\mu_u(a)t}. \quad (36)$$

  By the comparison principle applied to (34)–(35),

$$U_a(t) \le Z(t). \quad (37)$$

  Substituting (36) into (37) yields

$$U_a(t) \le \frac{\Lambda(a)}{\mu_u(a)} + \left(U_a(0) - \frac{\Lambda(a)}{\mu_u(a)}\right)e^{-\mu_u(a)t}. \quad (38)$$

  As the exponential factor decays to zero,

$$U_a(t) \le \frac{\Lambda(a)}{\mu_u(a)}, \qquad \forall t \ge 0. \quad (39)$$

- **Step 4:**

  Construction of the positively invariant region.

  Combining (32) and (39), the state remains in

$$\Omega = \left\{ \begin{array}{l} (M, L, A, D, U_a) : \\ 0 \le M, L, A, D \le N_{\max}, \\ 0 \le U_a \le \dfrac{\Lambda(a)}{\mu_u(a)},\ a \in [a_{\min}, a_{\max}] \end{array} \right\}. \quad (40)$$

  The vector field of the system points inward on the boundary of Ω, proving positive invariance of Ω.

□

6 Equilibrium Points

Consider the state vector

$$\mathbf{X}(t) = \big(M(t), L(t), A(t), D(t), U_a(t)\big)$$

representing the proportions of stable marriages, long-distance marriages, extramarital affairs, divorced individuals, and the age-structured unmarried women population, respectively.

An *equilibrium point* $\mathbf{X}^* = (M^*, L^*, A^*, D^*, U_a^*)$ satisfies the system

$$\frac{d\mathbf{X}}{dt} = \mathbf{0}.$$

Explicitly, $\mathbf{X}^*$ must satisfy the nonlinear algebraic system

$$\begin{cases} 0 = -\lambda M^* - \alpha_1 M^* \left(1 - \dfrac{A^*}{K}\right) + \delta L^* + \beta A^* \\ \qquad - \displaystyle\int_{a_{\min}}^{a_{\max}} \theta(a) U_a^* M^*\, da, \\ 0 = \lambda M^* - \delta L^* - \alpha_2 L^* \left(1 - \dfrac{A^*}{K}\right), \\ 0 = \alpha_1 M^* \left(1 - \dfrac{A^*}{K}\right) + \alpha_2 L^* \left(1 - \dfrac{A^*}{K}\right) \\ \qquad + \displaystyle\int_{a_{\min}}^{a_{\max}} \theta(a) U_a^* M^*\, da - (\beta + \gamma) A^*, \\ 0 = \gamma A^* + \mu M^*, \\ 0 = \Lambda(a) - \theta(a) U_a^* M^* - \mu_u(a) U_a^*, \quad \forall a \in [a_{\min}, a_{\max}]. \end{cases}$$

Theorem 6.1 (Existence of Equilibrium)**.** *Assuming all parameters are positive and bounded, and the functions $\theta(a), \Lambda(a), \mu_u(a)$ are continuous and positive over $[a_{\min}, a_{\max}]$, there exists at least one biologically meaningful equilibrium point $\mathbf{X}^*$ in the non-negative cone*

$$\{(M, L, A, D, U_a) \mid M, L, A, D \ge 0, \\ U_a \ge 0\ \forall a \in [a_{\min}, a_{\max}]\}.$$

Such an equilibrium corresponds to long-term steady-state proportions of the marital compartments and unmarried population under the modeled social dynamics.

Sketch. The system is composed of continuous nonlinear functions with biologically motivated positivity constraints. Compactness and continuity conditions, together with positivity of birth/inflow functions $\Lambda(a)$ and natural exit terms $\mu_u(a)$, ensure the existence of fixed points by standard application

of fixed-point theorems such as Brouwer or Schauder. Non-negativity follows from the positive invariance proved previously. The age-structured equation yields explicit expressions for U_a^* in terms of M^*, which reduces the problem to a finite-dimensional nonlinear algebraic system in M^*, L^*, A^*, D^*. Existence results for such systems under positivity and boundedness assumptions are classical. □

Lemma 6.2 (Existence of the Zero Equilibrium). *Define the trivial equilibrium candidate*

$$\mathbf{E}_0 := (M^*, L^*, A^*, D^*, U_a^*) = (0, 0, 0, 0, 0).$$

Then $\mathbf{E}_0$ is an equilibrium of the full five–compartment steady system (1)–(5) if and only if

$$\Lambda(a) \equiv 0, \qquad \forall\, a \in [a_{\min}, a_{\max}]. \tag{41}$$

Lemma 6.3 (Existence and form of the Age–only Equilibrium). *Let the steady system be given by equations (1)–(5). Define the age-only equilibrium candidate*

$$\mathbf{E}_1 := (M^*, L^*, A^*, D^*, U_a^*) = \Big(0, 0, 0, 0,\, U_a^*(a)\Big), \quad a \in [a_{\min}, a_{\max}],$$

where

$$U_a^*(a) \;=\; \frac{\Lambda(a)}{\mu_u(a)}. \tag{42}$$

Then $\mathbf{E}_1$ is an equilibrium of the full five–compartment system (1)–(5) if and only if $\Lambda(a) \geq 0$ for all a. Moreover, $\mathbf{E}_1$ is nontrivial (i.e. $U_a^*(a) > 0$ for some a) precisely when $\Lambda(a) > 0$ on a set of positive measure in $[a_{\min}, a_{\max}]$.

Lemma 6.4 (No–affair equilibrium $\mathbf{E}_2$). *Consider the steady system (1)–(5) and impose the condition $A^* = 0$. Then the steady relations imply*

$$M^* = 0, \qquad L^* = 0,$$

so that the only biologically admissible equilibrium with $A^* = 0$ and all parameters strictly positive is

$$\mathbf{E}_2 = (0, 0, 0, 0,\, U_a^*), \qquad U_a^* = \frac{\Lambda(a)}{\mu_u(a)},$$

which coincides with the age–only equilibrium $\mathbf{E}_1$. No additional nontrivial $A = 0$ equilibria exist unless one or more model parameters are degenerate (e.g. $\beta = 0$ or $\mu = 0$).

Lemma 6.5 (Boundary equilibrium with prescribed affair level $\mathbf{E}_3$). *Suppose the model formulation permits a fixed saturation level $A^* = K > 0$. Then the steady relations obtained from equations (1)–(5) determine the corresponding equilibrium components as*

$$M^* \;=\; D^* \;=\; \frac{\gamma}{\mu} K, \qquad L^* = 0,$$

and the age–structured variable satisfies

$$U_a^*(a) = \frac{\Lambda(a) - \theta(a) K\, M^*}{\mu_u(a)}, \qquad a \in [a_{\min}, a_{\max}].$$

This equilibrium is biologically admissible only if

$$\Lambda(a) > \theta(a)\, K\, M^* \qquad \forall\, a,$$

ensuring $U_a^*(a) > 0$ across all age classes.

Lemma 6.6 (Interior (fully endemic) equilibrium $\mathbf{E}_5$). *Assume the existence of an equilibrium with strictly positive components,*

$$M^* > 0, \qquad L^* > 0, \qquad A^* > 0,$$
$$D^* > 0, \quad U_a^*(a) > 0 \quad \forall a \in [a_{\min}, a_{\max}].$$

Then the steady system (1)–(5) uniquely determines each compartment as follows:

Divorced class:

$$D^* \;=\; \frac{\gamma}{\mu} A^*. \tag{43}$$

Age–structured class:

$$U_a^*(a) \;=\; \frac{\Lambda(a)}{\mu_u(a) + \theta(a) M^*}. \tag{44}$$

Long–distance class:

$$L^* \;=\; \frac{\lambda\, M^*}{\delta + \alpha_2\big(1 - A^*/K\big)}. \tag{45}$$

Affair class (from the A–equation):

$$A^* \;=\; \frac{\beta}{\mu} M^*. \tag{46}$$

Substituting (44)–(46) into the steady A-equation gives a single nonlinear scalar equation for the unknown $M^* > 0$:

$$f(M^*) \;=\; 0, \tag{47}$$

where

$$\begin{aligned} f(M) =& \alpha_1 M\left(1 - \frac{A(M)}{K}\right) + \alpha_2 L(M)\left(1 - \frac{A(M)}{K}\right) \\ &+ M \int_{a_{\min}}^{a_{\max}} \frac{\theta(a)\Lambda(a)}{\mu_u(a) + \theta(a) M}\, da \\ &- (\beta + \gamma)\, A(M), \end{aligned}$$

and

$$A(M) = \frac{\beta}{\mu} M, \qquad L(M) = \frac{\lambda M}{\delta + \alpha_2 \left(1 - A(M)/K\right)}.$$

Any strictly positive root $M^* > 0$ of (47) generates a full interior equilibrium via

$$A^* = \frac{\beta}{\mu} M^*, \qquad L^* = \frac{\lambda M^*}{\delta + \alpha_2 (1 - A^*/K)},$$
$$D^* = \frac{\gamma}{\mu} A^*, \qquad U_a^*(a) = \frac{\Lambda(a)}{\mu_u(a) + \theta(a) M^*}.$$

This equilibrium represents the unique fully interacting (endemic) state of the system when all components coexist at strictly positive levels.

7 Local Stability of Equilibrium Points

In this section we analyze the local behavior of the dynamical system near each equilibrium point. Local stability is determined by evaluating the Jacobian matrix at an equilibrium and studying the signs of its eigenvalues.

7.1 Jacobian of the complete system and local stability lemmas

Lemma 7.1 (Jacobian of the full system)**.** *Let the system variables be ordered as*

$$\mathbf{X} = \left(M,\ L,\ A,\ D,\ U_{a_1}, \ldots, U_{a_n}\right)^\top,$$

where the age interval $[a_{\min}, a_{\max}]$ is discretized into $\{a_1, \ldots, a_n\}$. The right–hand sides of the model are

$$\dot{\mathbf{X}} = \mathbf{F}(\mathbf{X}) = \left(F_M,\ F_L,\ F_A,\ F_D,\ F_{U_{a_1}}, \ldots, F_{U_{a_n}}\right)^\top,$$

with

$$F_M = -\lambda M - \alpha_1 M \left(1 - \frac{A}{K}\right) + \delta L + \beta A - M \sum_{i=1}^{n} \theta_i U_{a_i},$$

$$F_L = \lambda M - \delta L - \alpha_2 L \left(1 - \frac{A}{K}\right),$$

$$F_A = \alpha_1 M \left(1 - \frac{A}{K}\right) + \alpha_2 L \left(1 - \frac{A}{K}\right) + M \sum_{i=1}^{n} \theta_i U_{a_i} - (\beta + \gamma) A,$$

$$F_D = \gamma A + \mu M,$$

$$F_{U_{a_i}} = \Lambda_i - \theta_i M\, U_{a_i} - \mu_{u,i} U_{a_i}.$$

Then the Jacobian matrix

$$J(\mathbf{X}) = \frac{\partial \mathbf{F}}{\partial \mathbf{X}}$$

of the complete system has the block structure

$$J(\mathbf{X}) = \begin{pmatrix} J_{4\times 4} & J_{4\times n} \\ J_{n\times 4} & J_{n\times n} \end{pmatrix},$$

where the submatrices are described below.

(*i*) *The* 4×4 *subsystem Jacobian* (M, L, A, D)*:

$$J_{4\times 4} = \begin{pmatrix} -\lambda - \alpha_1\left(1 - \frac{A}{K}\right) - \sum \theta_i U_{a_i} & \delta & \alpha_1 \frac{M}{K} + \beta & 0 \\ \lambda & -\delta - \alpha_2\left(1 - \frac{A}{K}\right) & \alpha_2 \frac{L}{K} & 0 \\ \alpha_1\left(1 - \frac{A}{K}\right) + \alpha_2\left(1 - \frac{A}{K}\right) + \sum \theta_i U_{a_i} & \alpha_2\left(1 - \frac{A}{K}\right) & -\frac{\alpha_1 M}{K} - \frac{\alpha_2 L}{K} - (\beta + \gamma) & 0 \\ \mu & 0 & \gamma & 0 \end{pmatrix}$$

(*ii*) *Coupling of* (M, L, A, D) *with the age subsystem:*

$$(J_{4\times n})_{1,i} = -M\theta_i, \qquad (J_{4\times n})_{3,i} = M\theta_i,$$
all other rows zero.

(*iii*) *Effect of* (M, L, A, D) *on the age classes:*

$$(J_{n\times 4})_{i,1} = -\theta_i U_{a_i}, \qquad (J_{n\times 4})_{i,2} = 0,$$
$$(J_{n\times 4})_{i,3} = 0, \qquad (J_{n\times 4})_{i,4} = 0.$$

(*iv*) *Age–structured block* $J_{n\times n}$*:

$$(J_{n\times n})_{ii} = -\theta_i M - \mu_{u,i}, \qquad (J_{n\times n})_{ij} = 0\ (i \neq j).$$

Evaluating $J(\mathbf{X})$ at any equilibrium $\mathbf{X}^*$ yields the linearized dynamics

$$\dot{\mathbf{Z}} = J(\mathbf{X}^*)\, \mathbf{Z},$$

so that the equilibrium $\mathbf{X}^*$ is

- locally asymptotically stable *if all eigenvalues of $J(\mathbf{X}^*)$ have negative real parts,*
- unstable *if at least one eigenvalue has positive real part.*

Lemma 7.2 (Jacobian at the trivial equilibrium $\mathbf{E}_0$)**.** *Consider the full five–compartment system (1)–(5) and the trivial equilibrium*

$$\mathbf{E}_0 = (M^*, L^*, A^*, D^*, U_a^*) = (0, 0, 0, 0, 0).$$

Assume $\mu_u(a) > 0$ for all $a \in [a_{\min}, a_{\max}]$. The Jacobian matrix $J(\mathbf{X})$ evaluated at $\mathbf{E}_0$ has the block form

$$J(\mathbf{E}_0) = \begin{pmatrix} J_4^0 & \mathbf{0}_{4\times n} \\ \mathbf{0}_{n\times 4} & J_n^0 \end{pmatrix}, \tag{48}$$

where the 4×4 block J_4^0 (ordering (M, L, A, D)) is

$$J_4^0 = \begin{pmatrix} -\lambda - \alpha_1 & \delta & \beta & 0 \\ \lambda & -\delta - \alpha_2 & 0 & 0 \\ \alpha_1 + \alpha_2 & \alpha_2 & -(\beta + \gamma) & 0 \\ \mu & 0 & \gamma & 0 \end{pmatrix}, \tag{49}$$

and the age–structured block J_n^0 is diagonal with entries

$$(J_n^0)_{ii} = -\mu_u(a_i) \quad (i = 1, \ldots, n), \tag{50}$$

(or, in the continuum notation, the age operator is multiplication by $-\mu_u(a)$).

Consequently the spectrum of $J(\mathbf{E}_0)$ is the union of the spectrum of J_4^0 and the set $\{-\mu_u(a_i)\}_{i=1}^n$. In particular, if $\Re(\lambda_j(J_4^0)) < 0$ for every eigenvalue λ_j of J_4^0 and $\mu_u(a) > 0$ for all a, then all eigenvalues of $J(\mathbf{E}_0)$ have strictly negative real parts and hence $\mathbf{E}_0$ is locally asymptotically stable. If J_4^0 possesses at least one eigenvalue with positive real part, then $\mathbf{E}_0$ is unstable.

Proof. Evaluate the general Jacobian given in Lemma 7.1 at the state $M = L = A = D = 0$ and $U_a = 0$. All coupling terms that involve products M, L, A, or MU_a vanish at $\mathbf{E}_0$. In particular the off–diagonal coupling blocks $J_{4\times n}$ and $J_{n\times 4}$ are identically zero at $\mathbf{E}_0$, which yields the block form (48).

Direct substitution into the entries of the 4×4 block (see the general expressions in Lemma 7.1) produces (49). The age–block reduces to diagonal entries $-\mu_u(a_i)$ (or $-\mu_u(a)$ in continuum form), giving (50).

Since the full Jacobian is block–diagonal at $\mathbf{E}_0$, its spectrum is the union of the spectra of the diagonal blocks. The age–block contributes eigenvalues $-\mu_u(a_i)$, which lie strictly in the left half-plane by the assumption $\mu_u(a) > 0$. Therefore the sign of the real parts of the full spectrum is determined entirely by the eigenvalues of J_4^0. The stated stability/instability conclusions follow immediately from the linearization principle. □

Lemma 7.3 (Characteristic polynomial at $\mathbf{E}_0$)**.** *Let J_4^0 be the 4×4 Jacobian block at the trivial equilibrium $\mathbf{E}_0$ given in Lemma 7.2:*

$$J_4^0 = \begin{pmatrix} -\lambda - \alpha_1 & \delta & \beta & 0 \\ \lambda & -\delta - \alpha_2 & 0 & 0 \\ \alpha_1 + \alpha_2 & \alpha_2 & -(\beta + \gamma) & 0 \\ \mu & 0 & \gamma & 0 \end{pmatrix}.$$

Denote by $\chi_{J_4^0}(s) = \det(sI_4 - J_4^0)$ its characteristic polynomial. Then $\chi_{J_4^0}$ factors as

$$\chi_{J_4^0}(s) = s\,\big(s^3 + c_1 s^2 + c_2 s + c_3\big), \tag{51}$$

where the coefficients c_1, c_2, c_3 are given by

$$c_1 = \lambda + \alpha_1 + \delta + \alpha_2 + \beta + \gamma, \tag{52}$$

$$c_2 = (\lambda\alpha_2 + \alpha_1\delta + \alpha_1\alpha_2) + (\beta + \gamma)(\lambda + \alpha_1 + \delta + \alpha_2) - \beta(\alpha_1 + \alpha_2), \tag{53}$$

$$c_3 = (\beta + \gamma)\,(\lambda\alpha_2 + \alpha_1\delta + \alpha_1\alpha_2) - \beta\lambda\alpha_2 - \beta(\alpha_1 + \alpha_2)(\delta + \alpha_2). \tag{54}$$

In particular, the full characteristic polynomial of the Jacobian $J(\mathbf{E}_0)$ (including the age–structured block) is

$$\chi_{J(\mathbf{E}_0)}(s) = \chi_{J_4^0}(s) \prod_{i=1}^{n} (s + \mu_u(a_i)),$$

so the eigenvalues of $J(\mathbf{E}_0)$ consist of the roots of $s(s^3 + c_1 s^2 + c_2 s + c_3) = 0$ together with the age–block eigenvalues $-\mu_u(a_i)$.

What we aim to show in this subsection is the following:

> *Determine conditions on the model parameters under which all roots of the cubic factor of the characteristic polynomial*
>
> $$p(s) = s^3 + c_1 s^2 + c_2 s + c_3$$
>
> *have strictly negative real parts. In particular we apply the Routh–Hurwitz test to obtain algebraic inequalities in the parameters that guarantee local linear stability of the (M, L, A, U)–modes at the trivial equilibrium $\mathbf{E}_0$.*

Recall the parameter expressions (repeated for convenience):

$$c_1 = \lambda + \alpha_1 + \delta + \alpha_2 + \beta + \gamma, \tag{55}$$

$$c_2 = \lambda\alpha_2 + \alpha_1\delta + \alpha_1\alpha_2 + (\beta + \gamma)(\lambda + \alpha_1 + \delta + \alpha_2) - \beta(\alpha_1 + \alpha_2), \tag{56}$$

$$c_3 = (\beta + \gamma)\,(\lambda\alpha_2 + \alpha_1\delta + \alpha_1\alpha_2) - \beta\lambda\alpha_2 - \beta(\alpha_1 + \alpha_2)(\delta + \alpha_2). \tag{57}$$

Routh–Hurwitz criterion. The cubic polynomial $p(s)$ has all roots with strictly negative real parts iff the following four inequalities hold:

$$c_1 > 0, \qquad c_2 > 0, \qquad c_3 > 0, \qquad c_1 c_2 - c_3 > 0. \tag{58}$$

As noted previously, $c_1 > 0$ holds automatically for nonnegative parameters not all zero; the nontrivial checks are therefore the positivity of c_2, c_3 and the strict positivity of the Routh determinant $\Delta := c_1 c_2 - c_3$.

Algebraic expansion of the Routh determinant Δ. To make the dependence on the model parameters transparent we introduce the intermediate quantities

$$\begin{aligned} R :=& \lambda + \alpha_1 + \delta + \alpha_2, \\ S :=& c_1 = R + (\beta + \gamma), \\ T :=& \lambda\alpha_2 + \alpha_1\delta + \alpha_1\alpha_2. \end{aligned}$$

Using these definitions and substituting (56)-(57) we compute $\Delta = c_1 c_2 - c_3$ step by step. After straightforward algebra one obtains the compact form

$$\boxed{\begin{aligned} \Delta = & R\,T + (\beta+\gamma)\,S^2 \\ & - \beta\,S(\alpha_1+\alpha_2) + \beta\,\lambda\alpha_2 \\ & + \beta(\alpha_1+\alpha_2)(\delta+\alpha_2)\ . \end{aligned}} \tag{59}$$

Each monomial in (59) is nonnegative for nonnegative parameters, except that the third term appears with an explicit minus sign; expanding the formula recovers the original polynomial expression and shows exactly how the competing contributions combine.

Interpretation and "dangerous" parameter combinations.

- RT and $(\beta+\gamma)S^2$ are the dominant positive anchors in Δ. They grow when the transition rates $\lambda, \alpha_1, \alpha_2, \delta$ or the separation rate γ increase.
- The negative contribution $-\beta\,S(\alpha_1+\alpha_2)$ scales with β and $\alpha_1+\alpha_2$. Hence large values of both the extramarital initiation rate β and the instability rates α_1, α_2 tend to reduce Δ and are potentially destabilising.
- The remaining β-weighted positive terms, $\beta\lambda\alpha_2$ and $\beta(\alpha_1+\alpha_2)(\delta+\alpha_2)$, partially offset the negative term; therefore the net effect of increasing β depends on the relative sizes of these terms.
- **Practical rule of thumb:** combinations with relatively small R and T (i.e. small marriage/transition rates) together with large β and large $\alpha_1+\alpha_2$ are the most likely to violate $\Delta > 0$.

Usage and numerical recommendation.

1. For any chosen parameter set evaluate c_1, c_2, c_3 via (55)–(57) and compute Δ from (59). If $\Delta > 0$ and $c_2, c_3 > 0$, then the cubic is stable (all roots in the open left half-plane).
2. Because the expressions are multilinear and contain cancellations, a robust way to visualise dangerous regions is to perform two–parameter sweeps (e.g. β vs. $\alpha_1+\alpha_2$) and plot the sign of Δ. This reveals parameter regimes where the Routh inequality fails.
3. Finally, recall that the full Jacobian at $\mathbf{E}_0$ contains an eigenvalue at zero (the D–direction) and the age-block eigenvalues $-\mu_u(a)$ which are negative when $\mu_u(a) > 0$. Thus, even when the cubic is Hurwitz (all negative roots) and $\mu_u(a) > 0$, the trivial equilibrium $\mathbf{E}_0$ remains *non–hyperbolic* due to the neutral D–mode; one may conclude Lyapunov stability of the zero equilibrium for the (M, L, A, U)–modes but not asymptotic stability in the full five-dimensional state space unless the model is amended (for example by adding a decay term $-\kappa D$ with $\kappa > 0$).

The algebraic expansion (59) therefore provides both a symbolic certificate useful for analytical reasoning and a practical testable formula for numerical exploration of the stability region in parameter space.

7.2 Full expansion of the Routh determinant $\Delta = c_1 c_2 - c_3$

Recall

$$\begin{aligned} c_1 &= \lambda + \alpha_1 + \delta + \alpha_2 + \beta + \gamma, \\ c_2 &= \lambda\alpha_2 + \alpha_1\delta + \alpha_1\alpha_2 + (\beta+\gamma)c_1 - \beta(\alpha_1+\alpha_2), \\ c_3 &= (\beta+\gamma)\,(\lambda\alpha_2 + \alpha_1\delta + \alpha_1\alpha_2) - \beta\lambda\alpha_2 \\ &\quad - \beta(\alpha_1+\alpha_2)(\delta+\alpha_2). \end{aligned}$$

For clarity we write Δ as the sum of five blocks obtained in the compact representation $\Delta = RT + (\beta+\gamma)S^2 - \beta S(\alpha_1+\alpha_2) + \beta\lambda\alpha_2 + \beta(\alpha_1+\alpha_2)(\delta+\alpha_2)$, where $R = \lambda + \alpha_1 + \delta + \alpha_2$, $S = c_1$, $T = \lambda\alpha_2 + \alpha_1\delta + \alpha_1\alpha_2$. Expanding each block yields the following explicit polynomial:

$$\begin{aligned}\Delta \;=\; & \lambda^2\alpha_2 + \lambda\alpha_1\delta + 2\lambda\alpha_1\alpha_2 + \alpha_1^2\delta + \alpha_1^2\alpha_2 + \lambda\delta\alpha_2 \\ & + \alpha_1\delta^2 + 2\alpha_1\alpha_2\delta + \lambda\alpha_2^2 + \alpha_1\alpha_2^2 \\ & + (\beta+\gamma)\big(\lambda^2 + \alpha_1^2 + \delta^2 + \alpha_2^2 + 2\lambda\alpha_1 + 2\lambda\delta + 2\lambda\alpha_2 \\ & \quad + 2\alpha_1\delta + 2\alpha_1\alpha_2 + 2\delta\alpha_2\big) \\ & + 2(\beta+\gamma)^2\big(\lambda + \alpha_1 + \delta + \alpha_2\big) + (\beta+\gamma)^3 \\ & - \beta(\alpha_1+\alpha_2)\big(\lambda + \alpha_1 + \delta + \alpha_2\big) - \beta^2(\alpha_1+\alpha_2) \\ & - \beta\gamma(\alpha_1+\alpha_2) \\ & + \beta\lambda\alpha_2 + \beta\alpha_1\delta + \beta\alpha_1\alpha_2 + \beta\alpha_2\delta + \beta\alpha_2^2.\end{aligned}$$

Lemma 7.4 (Local Stability of the Equilibrium). *Consider the linearization of the five–compartment system around an equilibrium point $\mathbf{X}^* = (M^*, L^*, A^*, D^*, U_a^*)$. The Jacobian evaluated at $\mathbf{X}^*$ contains a 3×3 demographic block with characteristic polynomial*

$$\lambda^3 + c_1\lambda^2 + c_2\lambda + c_3 = 0, \tag{60}$$

where $c_1, c_2, c_3 > 0$ are smooth functions of the parameters $\lambda, \alpha_1, \delta, \alpha_2, \beta, \gamma$.

The equilibrium $\mathbf{X}^*$ is locally asymptotically stable *if and only if the Routh–Hurwitz conditions*

$$c_1 > 0, \qquad c_2 > 0, \qquad c_3 > 0, \qquad c_1c_2 > c_3, \tag{61}$$

are satisfied. If any of these inequalities fails, then $\mathbf{X}^*$ is unstable.

In particular, the inequality $c_1c_2 > c_3$ determines the stability threshold and distinguishes stable parameter regimes from unstable ones, indicating whether small perturbations decay or grow over time.

Lemma 7.5 (Jacobian at the age-only equilibrium $\mathbf{E}_1$). *Let $\mathbf{E}_1 = (0, 0, 0, 0, U_a^*(a))$ be the age-only equilibrium of the full five–compartment system (1)–(5), where*

$$U_a^*(a) = \frac{\Lambda(a)}{\mu_u(a)}, \qquad a \in [a_{\min}, a_{\max}].$$

Define the scalar quantity

$$\Theta \;:=\; \int_{a_{\min}}^{a_{\max}} \theta(a)\, U_a^*(a)\, da \;=\; \int_{a_{\min}}^{a_{\max}} \frac{\theta(a)\,\Lambda(a)}{\mu_u(a)}\, da, \tag{62}$$

(or, in a discretized age representation with nodes a_i, $\Theta = \sum_i \theta_i\Lambda_i/\mu_{u,i}$).

Then the Jacobian $J(\mathbf{X})$ of the full system evaluated at $\mathbf{E}_1$ has the block structure

$$J(\mathbf{E}_1) = \begin{pmatrix} J^{(1)}_{4\times4} & \mathbf{0}_{4\times n} \\ J^{(1)}_{n\times4} & J^{(1)}_{n\times n} \end{pmatrix},$$

with the following blocks (ordering the first four state variables as (M, L, A, D)):

(i) The 4×4 block (rows/cols M, L, A, D):

$$J^{(1)}_{4\times4} = \begin{pmatrix} -\lambda - \alpha_1 - \Theta & \delta & \beta & 0 \\ \lambda & -\delta - \alpha_2 & 0 & 0 \\ \alpha_1 + \alpha_2 + \Theta & \alpha_2 & -(\beta+\gamma) & 0 \\ \mu & 0 & \gamma & 0 \end{pmatrix}.$$

(ii) The $4 \times n$ coupling block (from age classes to M, L, A, D):

$$J^{(1)}_{4\times n} = \mathbf{0}_{4\times n},$$

because each entry in that block is proportional to M^* and $M^* = 0$ at $\mathbf{E}_1$.

(iii) The $n \times 4$ coupling block (effect of M, L, A, D on age classes):

$$\big(J^{(1)}_{n\times4}\big)_{i,1} = -\theta(a_i)\, U_a^*(a_i) = -\theta(a_i)\frac{\Lambda(a_i)}{\mu_u(a_i)}, \qquad i = 1, \ldots, n,$$

and all other columns of $J^{(1)}_{n\times4}$ are zero.

(iv) The age–structured block:

$$J^{(1)}_{n\times n} = \operatorname{diag}\big(-\mu_u(a_1), \ldots, -\mu_u(a_n)\big),$$

(i.e. in the continuum limit the age operator is multiplication by $-\mu_u(a)$).

Because $J^{(1)}_{4\times n} = \mathbf{0}$, the full Jacobian at $\mathbf{E}_1$ is block lower–triangular and its spectrum is the union of the spectra of $J^{(1)}_{4\times4}$ and of $J^{(1)}_{n\times n}$. In particular the age–block contributes eigenvalues $-\mu_u(a_i)$ (or the function $-\mu_u(a)$ in the continuum), which lie strictly in the left half-plane provided $\mu_u(a) > 0$ for all a.

Let A_3 denote the top-left 3×3 principal submatrix of $J^{(1)}_{4\times4}$ corresponding to the (M, L, A) variables:

$$A_3 := \begin{pmatrix} -\lambda - \alpha_1 - \Theta & \delta & \beta \\ \lambda & -\delta - \alpha_2 & 0 \\ \alpha_1 + \alpha_2 + \Theta & \alpha_2 & -(\beta+\gamma) \end{pmatrix}.$$

Then $\det(sI_4 - J^{(1)}_{4\times4}) = s\det(sI_3 - A_3)$ and hence the characteristic polynomial of $J^{(1)}_{4\times4}$ factors as

$$\chi_{J^{(1)}_{4\times4}}(s) = s\big(s^3 + c_1s^2 + c_2s + c_3\big),$$

where the cubic coefficients are the standard coefficients of $\det(sI_3 - A_3)$*:*

$$c_1 = -\operatorname{tr}(A_3) = \lambda + \alpha_1 + \delta + \alpha_2 + \beta + \gamma + \Theta, \tag{63}$$

$$c_2 = \textit{sum of principal } 2\times 2 \textit{ minors of } A_3, \tag{64}$$

$$c_3 = -\det(A_3). \tag{65}$$

(Explicit algebraic expressions for c_2, c_3 *are obtained by evaluating the appropriate* 2×2 *minors and the determinant of* A_3*; they are multilinear polynomials in* $\{\lambda, \alpha_1, \delta, \alpha_2, \beta, \gamma\}$ *and in the aggregate* Θ *defined in* (62)*.)*

Stability conclusion.
Assume $\mu_u(a) > 0$ *for all* a*. Then* $\mathbf{E}_1$ *is locally (asymptotically) stable in the subspace spanned by* (M, L, A, U) *(and the age modes decay) if and only if the roots of the cubic*

$$s^3 + c_1 s^2 + c_2 s + c_3 = 0$$

have strictly negative real parts. By the Routh–Hurwitz criterion this is equivalent to

$$c_1 > 0, \qquad c_2 > 0, \qquad c_3 > 0, \qquad c_1 c_2 > c_3. \tag{66}$$

If these inequalities hold and $\mu_u(a) > 0$*, then all eigenvalues of* $J(\mathbf{E}_1)$ *lie in the closed left half-plane, with the age-modes strictly negative; note, however, that* $J^{(1)}_{4\times 4}$ *always contains the simple eigenvalue* $s = 0$ *coming from the* D*–equation (no self–decay of* D*), so* $\mathbf{E}_1$ *is* non-hyperbolic *in the full five-dimensional space and is Lyapunov stable but not asymptotically stable in the* D*-direction unless a decay term for* D *(e.g.* $-\kappa D$*) is introduced.*

Lemma 7.6 (Jacobian at the no–affair equilibrium $\mathbf{E}_2$)**.** *Consider the full five–compartment steady system* (1)–(5)*. Assume the parameter set satisfies* $\beta > 0$ *and* $\mu > 0$*. Impose the no–affair condition* $A^* = 0$*. Then, for standard (nondegenerate) parameters the steady relations force* $M^* = 0$ *and* $L^* = 0$*, and the age–structured equilibrium is*

$$U_a^*(a) = \frac{\Lambda(a)}{\mu_u(a)}, \qquad a \in [a_{\min}, a_{\max}].$$

Hence in the generic case the no–affair equilibrium coincides with the age–only equilibrium $\mathbf{E}_1$*; we denote this equilibrium by* $\mathbf{E}_2 = (0, 0, 0, 0, U_a^*(a))$*.*

Define the aggregation

$$\Theta := \int_{a_{\min}}^{a_{\max}} \theta(a)\, U_a^*(a)\, da = \int_{a_{\min}}^{a_{\max}} \frac{\theta(a)\,\Lambda(a)}{\mu_u(a)}\, da, \tag{67}$$

(or $\Theta = \sum_i \theta_i \Lambda_i / \mu_{u,i}$ *in the discrete age case).*

Then the Jacobian $J(\mathbf{X})$ *at* $\mathbf{E}_2$ *has the block form*

$$J(\mathbf{E}_2) = \begin{pmatrix} J^{(2)}_{4\times 4} & \mathbf{0}_{4\times n} \\ J^{(2)}_{n\times 4} & J^{(2)}_{n\times n} \end{pmatrix},$$

with the following blocks (ordering variables as (M, L, A, D)*):*

(i) The 4×4 ***block (rows/cols*** M, L, A, D***):***

$$J^{(2)}_{4\times 4} = \begin{pmatrix} -\lambda - \alpha_1 - \Theta & \delta & \beta & 0 \\ \lambda & -\delta - \alpha_2 & 0 & 0 \\ \alpha_1 + \alpha_2 + \Theta & \alpha_2 & -(\beta + \gamma) & 0 \\ \mu & 0 & \gamma & 0 \end{pmatrix}.$$

(ii) The $4 \times n$ ***block:*** $J^{(2)}_{4\times n} = \mathbf{0}$*, since each entry there is proportional to* M^* *(and* $M^* = 0$*).*

(iii) The $n \times 4$ ***block:***

$$\big(J^{(2)}_{n\times 4}\big)_{i,1} = -\theta(a_i)\, U_a^*(a_i) = -\theta(a_i)\frac{\Lambda(a_i)}{\mu_u(a_i)}, \qquad i = 1, \ldots, n,$$

all other columns are zero.

(iv) The age–block:

$$J^{(2)}_{n\times n} = \operatorname{diag}\big(-\mu_u(a_1), \ldots, -\mu_u(a_n)\big),$$

(i.e. multiplication by $-\mu_u(a)$ *in the continuum).*

Because $J^{(2)}_{4\times n} = \mathbf{0}$*, the full Jacobian is block lower–triangular and its eigenvalues are the union of the eigenvalues of* $J^{(2)}_{4\times 4}$ *and the age–block eigenvalues* $-\mu_u(a_i)$*. Thus, provided* $\mu_u(a) > 0$ *for all* a*, the age modes lie strictly in the left half-plane and stability reduces to the spectral properties of the* 4×4 *block.*

Let $A^{(2)}_3$ *denote the principal* 3×3 *submatrix of* $J^{(2)}_{4\times 4}$ *corresponding to* (M, L, A)*. Then*

$$\det(sI_4 - J^{(2)}_{4\times 4}) = s\det\big(sI_3 - A^{(2)}_3\big),$$

and the characteristic cubic for the demographic modes is

$$s^3 + c_1 s^2 + c_2 s + c_3 = 0,$$

with coefficients c_1, c_2, c_3 *depending on* $\lambda, \alpha_1, \delta, \alpha_2, \beta, \gamma$ *and the aggregate* Θ *(analogous to the expressions in Lemma* 7.5 *but with* Θ *fixed by* (67)*).*

Stability criterion. *Assume $\mu_u(a) > 0$ for all a. Then $\mathbf{E}_2$ is locally asymptotically stable (in the (M, L, A, U) subspace) if and only if the Routh–Hurwitz conditions for the cubic hold:*

$$c_1 > 0, \qquad c_2 > 0, \qquad c_3 > 0, \qquad c_1 c_2 > c_3.$$

If any of these inequalities fails, $\mathbf{E}_2$ is unstable.

Degenerate cases. *If one or more parameters are degenerate (for example $\beta = 0$ or $\mu = 0$), then the algebraic relations leading to $M^* = 0$, $L^* = 0$ may change and additional equilibrium branches (e.g. $M > 0$ with $A = 0$) must be analyzed separately; the Jacobian formula above must be adapted to those parameter-specialized equilibria.*

8 Results and Discussions

In this section we examine the numerical behaviour of system (1)–(5) under variation of the affair–formation rate α_1. Unless otherwise stated, all simulations were performed on the interval $t \in [0, 100]$ with the fixed parameter set

$$\begin{aligned} &\alpha_2 = 0.08, \quad \beta = 0.03, \quad \gamma = 0.04, \\ &\mu = 0.01, \quad \lambda = 0.02, \quad \delta = 0.01, \quad K = 1. \end{aligned}$$

The age–dependent functions were taken as

$$\theta(a) = \frac{\exp\left[-\frac{(a-25)^2}{2\sigma^2}\right]}{\sum_{j=18}^{40} \exp\left[-\frac{(j-25)^2}{2\sigma^2}\right]}, \qquad \Lambda(a) = 10^{-3},$$
$$\mu_u(a) = 0.01,$$

for all integer ages $18 \le a \le 40$, with $\sigma = 4$. The initial conditions were chosen as

$$\begin{aligned} &M(0) = 0.8, \qquad L(0) = 0.1, \qquad A(0) = 0.05, \\ &D(0) = 0, \qquad U_a(0) = 0.01, \end{aligned}$$

representing an initially stable marriage-dominated population with a uniform unmarried age distribution.

8.1 Impact of the Affair–Formation Rate α_1 on Social Compartments

Figure 3 illustrates the temporal evolution of the four social compartments $M(t)$, $L(t)$, $A(t)$, and $D(t)$ under three representative instability levels $\alpha_1 \in \{0.03, 0.05, 0.08\}$. As α_1 increases, transitions from stable marriage to extramarital involvement occur more rapidly, leading to a noticeably faster decline in the married population $M(t)$. The long–distance compartment $L(t)$ also decreases, reflecting reduced stability before couples separate geographically. In contrast, the affairs class $A(t)$ rises more sharply and attains an earlier peak for larger α_1 values, indicating intensification of extramarital activity. This, in turn, drives a quicker and larger accumulation of divorced individuals $D(t)$. Overall, the parameter α_1 acts as a strong instability driver: increasing its value accelerates the breakdown of stable marriages and amplifies the subsequent rise in both affairs and divorce rates. rriages and increase the flow into divorce.

8.2 Impact of α_1 on the Age-Structured Unmarried Population

The surfaces displayed in Figure 4 illustrate how the unmarried population

$$U(t) = \sum_{a=18}^{40} \theta(a) U_a(t)$$

depends jointly on time and the instability parameter. For each value of α_1, the total unmarried population increases monotonically in time; moreover, the magnitude of $U(t)$ increases strictly with α_1. This confirms that higher marital instability causes stronger demographic inflow into the unmarried class. The full age–time surfaces $U(a, t)$ also exhibit clear structure. The largest densities occur around ages 25–32, coinciding with the peak of the interaction kernel $\theta(a)$ that governs social exposure and engagement probability. As α_1 increases, this concentration intensifies, producing sharper ridges in the (a, t) plane corresponding to younger unmarried individuals.

Remark 8.1 (Summary of the Effect of α_1)**.** *An increase in the instability parameter α_1 produces a pronounced amplification of the social dynamics within the system. Higher values of α_1 accelerate the flow from stable marriage into extramarital involvement, which in turn speeds up the transition from affairs to divorce. This chain reaction raises both the overall magnitude of the unmarried population and the concentration of unmarried individuals within key age intervals. Consequently, α_1 acts as a highly sensitive behavioural driver whose escalation can trigger significant demographic shifts and destabilise long-term marital structures.*

8.3 Sensitivity Analysis of Model Parameters

The parameter–sensitivity analysis, illustrated in Figures 5 and 6, demonstrates how variations in the transition rates shape the long-term behaviour of the unmarried population $U(t)$. The 3D surfaces indicate that increasing the marriage-to-affair transition rate α_1 or the instability rate within long-distance

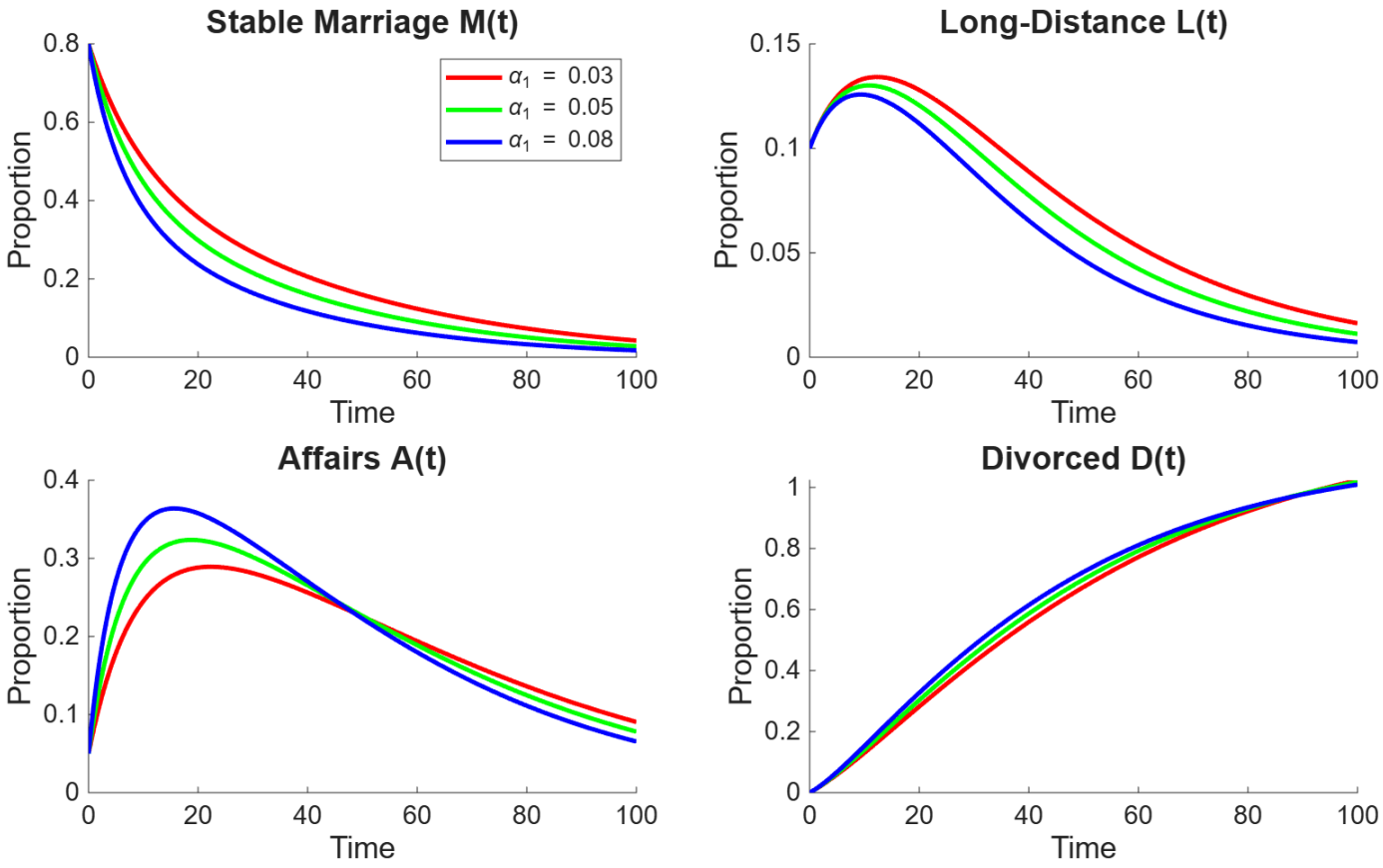

Figure 3. Time evolution of the four marital compartments under varying values of the transition rate α_1 for $M(t)$, $L(t)$, $A(t)$, and $D(t)$ over the time interval $t \in [0, 100]$ for three values of the marriage-to-affair transition rate are investigated: $\alpha_1 = 0.03$ (red), $\alpha_1 = 0.05$ (green), and $\alpha_1 = 0.08$ (blue). Other parameters are fixed at $\alpha_2 = 0.08$, $\beta = 0.03$, $\gamma = 0.04$, $\mu = 0.01$, $\lambda = 0.02$, $\delta = 0.01$, and $K = 1$.

relationships α_2 substantially accelerates the growth of $U(t)$, confirming that relationship instability is a primary driver of unmarried population expansion. Likewise, a larger extramarital formation rate β amplifies $U(t)$ by strengthening inflow into the affairs compartment, while a higher separation pressure γ increases divorce outflow and thus contributes to persistent growth in $U(t)$.

In contrast, the demographic removal rate μ produces a clear suppressing effect: higher values slow the increase of $U(t)$ by removing individuals from the marital classes. The transition rates λ (movement from marriage to long-distance) and δ (reunification from long-distance to marriage) exhibit comparatively weaker influence, modifying the curvature of $U(t)$ rather than its long-term levels. The 2D line plots reinforce these observations, showing nearly linear separation between curves corresponding to the strongly influential parameters $\alpha_1, \alpha_2, \beta$, and γ, whereas the curves for λ and δ remain tightly clustered.

Overall, the combined evidence indicates that relationship instability and extramarital involvement exert the strongest influence on the unmarried population, while movement between the married and long-distance compartments plays a secondary but still measurable role in shaping the demographics.

8.4 Parameter Sensitivity and Its Influence on the Unmarried Population

To quantify how behavioural and demographic parameters shape the long-term distribution of the population, we examined the response of the total unmarried population $U(t)$ under systematic variation of each transition rate. Figure 7 displays three-dimensional surfaces of $U(t)$ over the time interval $0 \leq t \leq 100$, generated by varying α_1, α_2, β, γ, μ, λ, and δ across representative low, medium, and high values, while keeping all other parameters fixed at their baseline levels. Several clear patterns emerge from these simulations. First, parameters associated with relationship instability—namely α_1 (marriage-to-affair transition), α_2 (long-distance deterioration), and β (initiation of extramarital relationships)—produce substantial increases in $U(t)$ as they grow. Higher values of these parameters

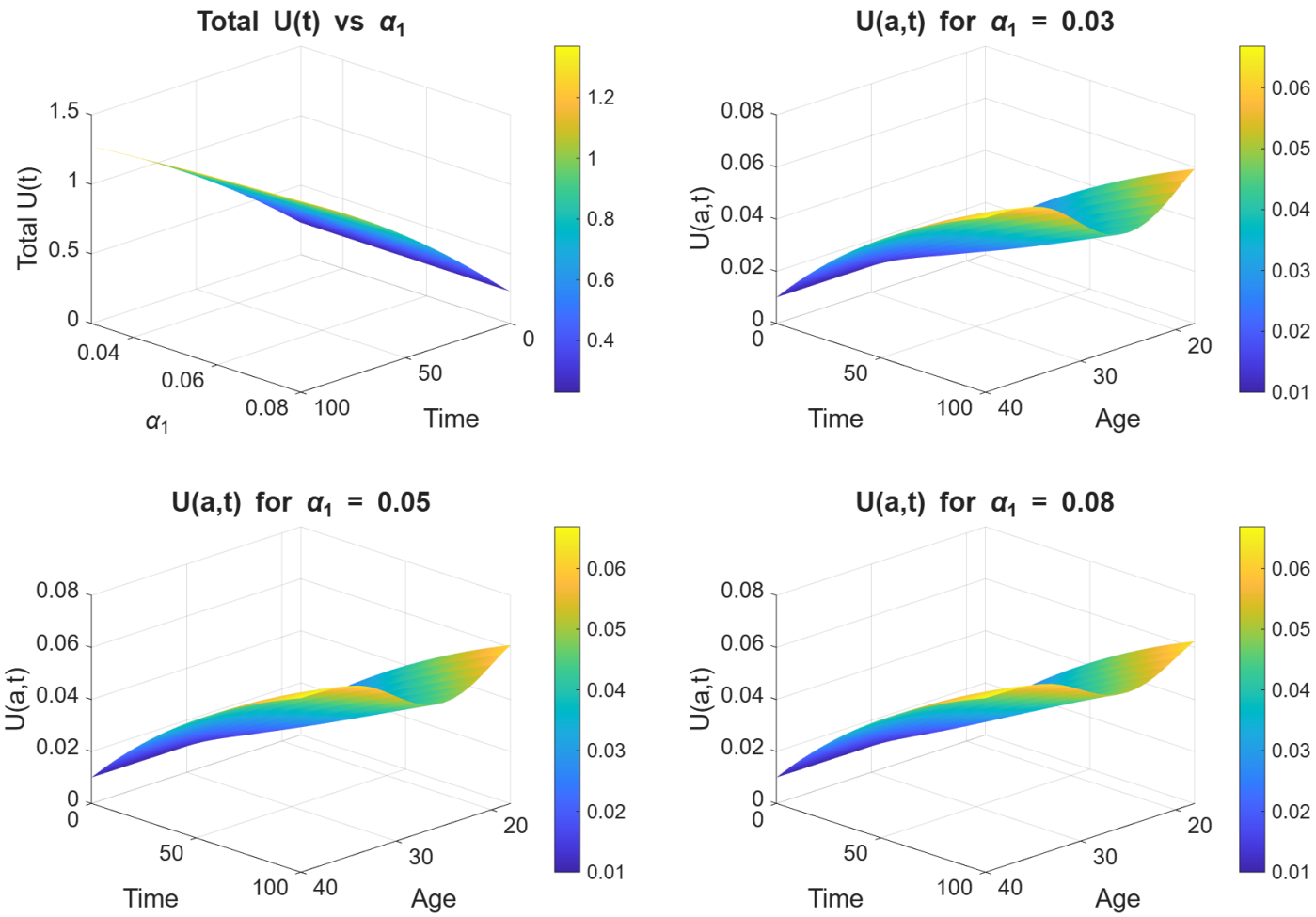

Figure 4. 3D surfaces of unmarried population dynamics for varying α_1.

lead to more rapid expansion of the unmarried population and elevated long-term levels, confirming that instability within either marital or long-distance partnerships is the dominant mechanism driving the enlargement of the unmarried class. Second, the separation parameter γ exerts a similarly strong influence, since increases in breakup pressure directly raise the inflow into the divorced class. In contrast, the demographic removal rate μ produces a dampening effect: larger μ values slow the growth of $U(t)$ and reduce its long-term amplitude, indicating that mortality or out-migration acts to partially counterbalance the effects of social instability. Finally, the parameters governing transitions between the married and long-distance states (λ and δ) exhibit comparatively weaker but still measurable effects. Their influence primarily modifies the curvature and slope of $U(t)$, rather than dramatically altering long-term levels, suggesting that geographical separation and reunification processes play a secondary role relative to behavioural instability.

Overall, the sensitivity analysis demonstrates that relationship-instability parameters (α_1, α_2, β, and γ) are the most significant determinants of unmarried population growth, while demographic turnover (μ) and spatial-transition mechanisms (λ, δ) provide moderating effects. These findings emphasize the pathways through which interpersonal behaviour translates into long-term demographic patterns at the population scale.

Figure 8 presents a comprehensive sensitivity analysis of the system with respect to the divorce–transition parameter γ and the marriage–formation parameter λ, evaluated at the long-term time horizon $t = 100$. The 2D curves in the left column reveal that increasing γ consistently decreases the levels of stable marriages $M(t)$ and long-distance relationships $L(t)$, while simultaneously increasing the divorced population $D(t)$. This behaviour is intuitive, as a higher divorce rate accelerates departures from the marriage compartment and accumulates individuals into the divorced class. The affairs compartment $A(t)$ exhibits a weaker but still monotonic decline with increasing γ, reflecting the fact that higher breakup

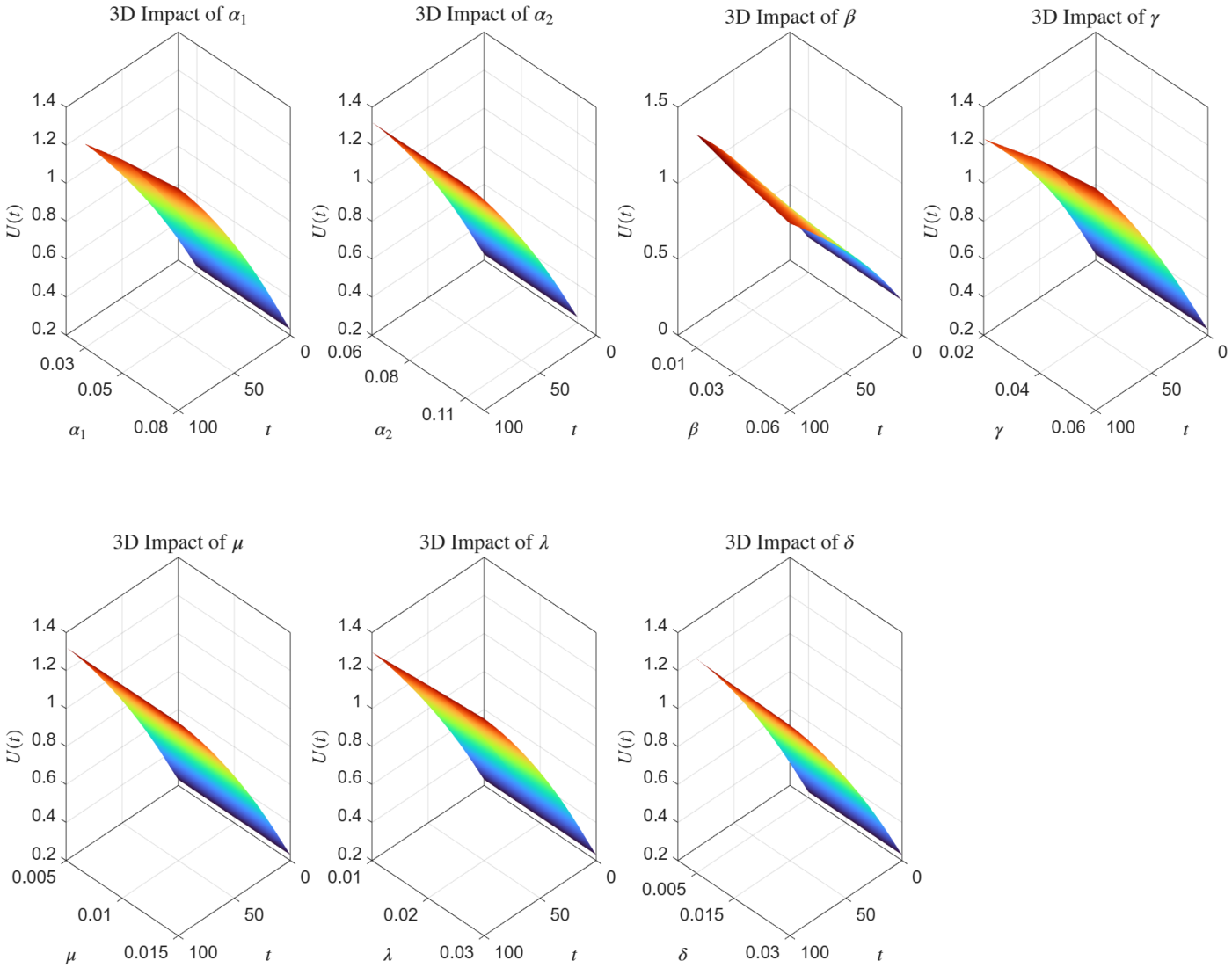

Figure 5. Three–dimensional surface plots illustrating the effect of each model parameter α_1, α_2, β, γ, μ, λ, and δ on the total unmarried population $U(t) = \sum_a U(a,t)$ over the time horizon $t \in [0, 100]$. For each parameter, three representative values were used: $\alpha_1 \in \{0.03, 0.05, 0.08\}$, $\alpha_2 \in \{0.06, 0.08, 0.11\}$, $\beta \in \{0.01, 0.03, 0.06\}$, $\gamma \in \{0.02, 0.04, 0.06\}$, $\mu \in \{0.005, 0.010, 0.015\}$, $\lambda \in \{0.01, 0.02, 0.03\}$, $\delta \in \{0.005, 0.015, 0.03\}$. All other parameters were held fixed at their baseline values: $\alpha_1 = 0.05$, $\alpha_2 = 0.08$, $\beta = 0.03$, $\gamma = 0.04$, $\mu = 0.01$, $\lambda = 0.02$, $\delta = 0.01$, $K = 1$; and age–structured terms were set as $\theta(a) = \exp(-(a-25)^2/32)$ (normalized), $\Lambda(a) = 10^{-3}$, and $\mu_u(a) = 0.01$ for $a = 18, \ldots, 40$. The surfaces demonstrate how parameter variations modulate the overall growth and curvature of $U(t)$, revealing nonlinear sensitivity in the population dynamics.

rates reduce the persistence of affairs over long time scales. The influence of the marriage–formation parameter λ is visible through the three curves in each 2D plot: larger values of λ increase $M(t)$ and $A(t)$ at $t = 100$, while suppressing $L(t)$ due to faster transitions from premarital states into the married class. The 3D surface plots in the middle column further illustrate these trends over the full (γ, λ) parameter plane. These surfaces display smooth curvature, showing that the combined nonlinear effects of the parameters are not additive: variations in γ have stronger impact when λ is small, whereas the effect of λ saturates as γ becomes large. Finally, the contour plots in the right column highlight the geometry of the parameter response landscape. The contours for M and L decrease along the γ–direction, while the contours for D increase, confirming the expected monotonic behaviour seen in the 2D and 3D views. Overall, the combined analysis demonstrates that (γ, λ) jointly control the long-term distribution of marital states, with γ acting as a destabilising force that amplifies divorce levels, and λ serving as a stabilising parameter that strengthens marriage formation and reduces long-distance relationships.

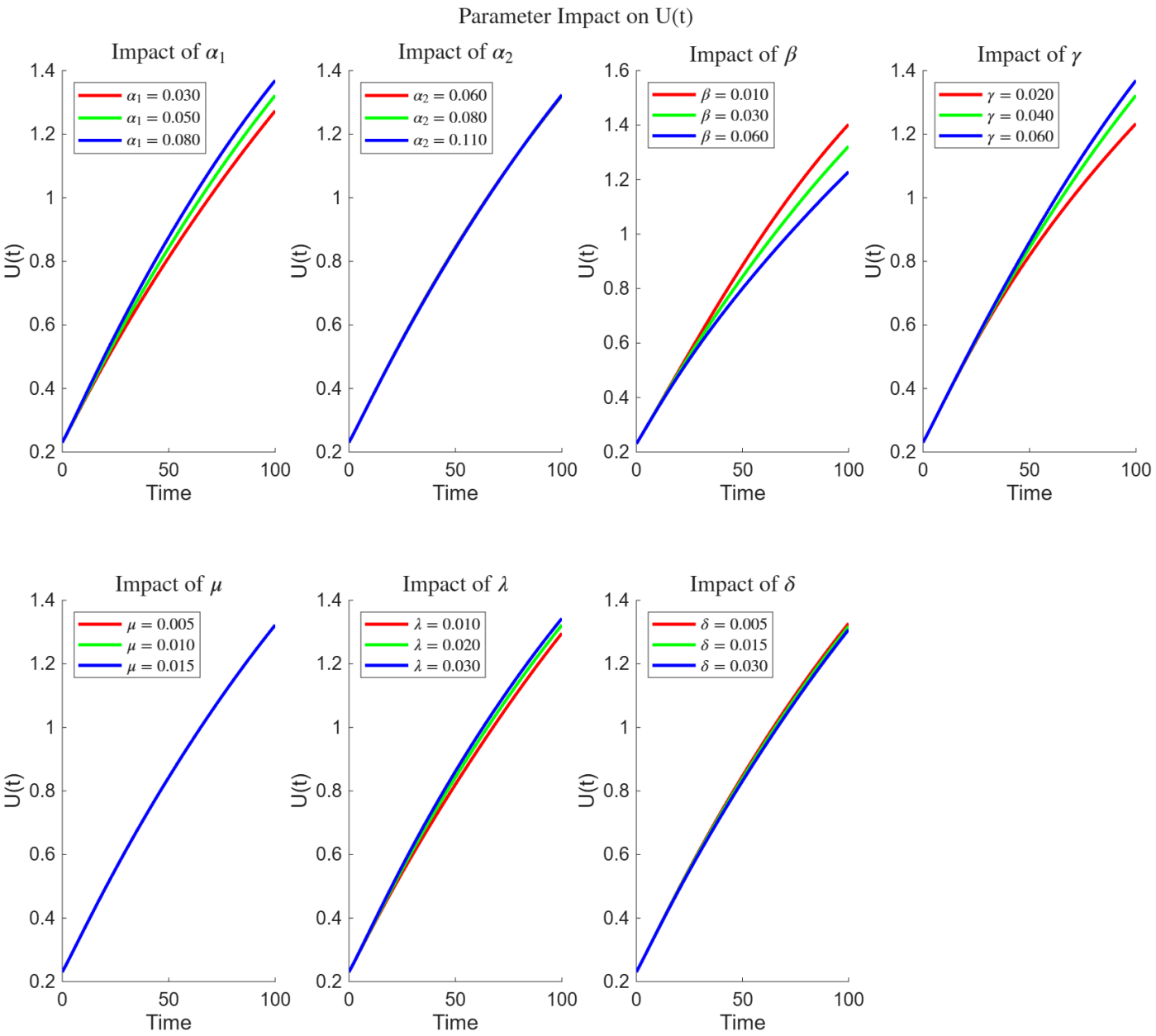

Figure 6. Two–dimensional sensitivity plots showing the temporal evolution of the total unmarried population $U(t)$ under variations of the parameters α_1, α_2, β, γ, μ, λ, and δ. Each panel corresponds to one parameter, where three representative values are simulated while keeping all remaining parameters fixed at their baseline values: $\alpha_1 = 0.05$, $\alpha_2 = 0.08$, $\beta = 0.03$, $\gamma = 0.04$, $\mu = 0.01$, $\lambda = 0.02$, $\delta = 0.01$, and $K = 1$. Age–dependent functions are identical to Figure 5. The curves reveal how each parameter influences the rate of increase and final magnitude of $U(t)$, allowing direct comparison of sensitivity across model components.

8.5 Two-Parameter Sensitivity Analysis with Respect to μ and K

Figure 9 presents a smooth two-parameter sensitivity study of the marital dynamics with respect to the dissolution parameter μ and the saturation parameter K, evaluated at the long-time state $t = 100$. The left column shows two-dimensional profiles of the social compartments $M(t)$, $L(t)$, $A(t)$, and $D(t)$ plotted against μ for three fixed values of $K \in \{0.8, 1.0, 1.2\}$. Across the compartments M, L, and A, the curves vary only mildly with μ, indicating that the dissolution rate has a relatively weak effect on the marital structure compared with other instability parameters. In contrast, increasing the saturation level K systematically elevates both $M(t)$ and $A(t)$ while reducing $L(t)$, revealing that a larger K—interpreted as a higher tolerance for extramarital involvement—introduces a slight stabilisation in the marriage–affair interaction. The divorced population $D(t)$, however, grows almost linearly with μ, reflecting the direct contribution of the term μM to the

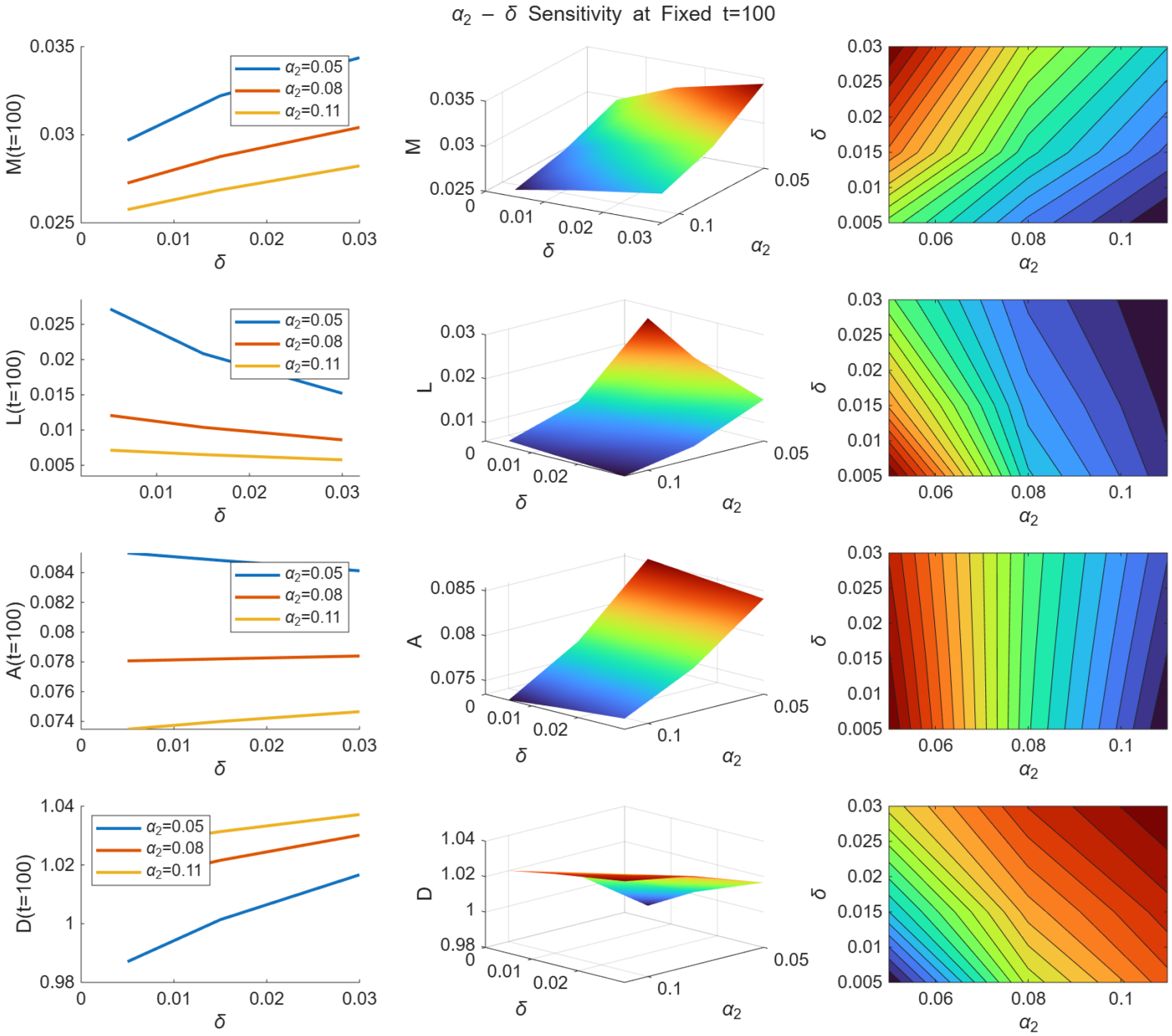

Figure 7. Three-dimensional sensitivity surfaces showing the effect of key model parameters α_1, α_2, β, γ, μ, λ, and δ on the total unmarried population $U(t)$ over the time interval $t \in [0, 100]$. Each panel varies the corresponding parameter across three representative values, while all other parameters are held at their baseline levels: $\alpha_1 = 0.05$, $\alpha_2 = 0.08$, $\beta = 0.03$, $\gamma = 0.04$, $\mu = 0.01$, $\lambda = 0.02$, $\delta = 0.01$, and $K = 1$. Age-structured functions follow $\theta(a) = \exp(-(a-25)^2/(2\sigma^2))$ (normalized), $\Lambda(a) = 10^{-3}$ and $\mu_u(a) = 0.01$ for $a = 18, \ldots, 40$. The surfaces illustrate how parameter variations influence the nonlinear trajectories of $U(t)$, identifying which behavioral and demographic factors most strongly affect system evolution.

divorce compartment. The central column displays the corresponding three-dimensional surfaces of the mapping $(\mu, K) \mapsto X(t)$ for each compartment. For M, L, and A, the surfaces vary primarily along the K-axis, confirming that K is the dominant driver of these compartments. Conversely, the D-surface varies most steeply along the μ-axis, providing a geometric verification that dissolution pressure overwhelmingly governs the size of the divorced population. The right-column contour plots further clarify these observations. For the compartments M, L, and A, the contour lines are nearly horizontal, indicating that level sets depend strongly on K and only weakly on μ. In contrast, the contour map for D exhibits pronounced vertical gradients, demonstrating that changes in μ induce substantial variation in the long-term divorced population. Taken together, the 2D profiles, 3D surfaces, and contour maps reveal a clear and interpretable parameter separation: the saturation parameter K primarily regulates the marriage-related

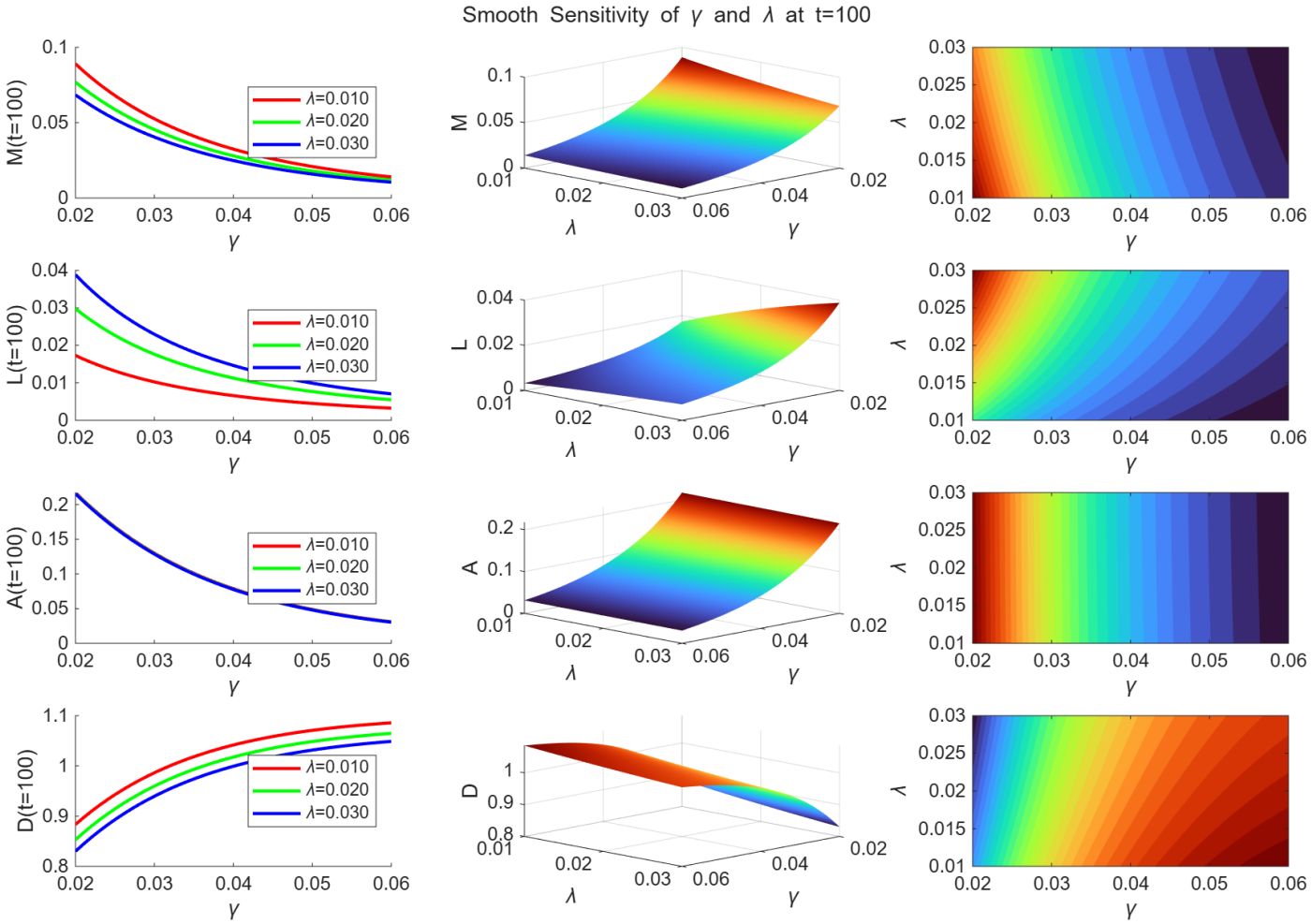

Figure 8. Sensitivity analysis of the divorce–marriage system with respect to the interaction parameter γ and the marriage–formation parameter λ evaluated at $t = 100$. The left column shows smooth 2D curves of each compartment $M(t)$, $L(t)$, $A(t)$, and $D(t)$ as a function of γ for three fixed values of $\lambda \in \{0.01, 0.02, 0.03\}$. The middle column shows corresponding 3D surface plots of $\lambda \times \gamma$ against the terminal values of each compartment, while the right column presents filled contour plots for the same parameter domain. The baseline parameter values used for all simulations are: $\alpha_1 = 0.05$, $\alpha_2 = 0.08$, $\beta = 0.03$, $\gamma \in [0.02, 0.06]$, $\mu = 0.01$, $\lambda \in [0.01, 0.03]$, $\delta = 0.01$, $K = 1$, with initial conditions $(M(0), L(0), A(0), D(0)) = (0.8,\ 0.1,\ 0.05,\ 0)$ and $U(a, 0) = 0.01$ for all $a \in [18, 40]$.

compartments (M, L, A), whereas the dissolution parameter μ almost exclusively determines the long-term behaviour of the divorced population $D(t)$. This structural asymmetry reflects the model's design, in which μ acts as a direct source term for divorce, while K modulates the nonlinear interactions that govern marital stability and the formation of affairs.

9 Overall Conclusion

The qualitative analysis of the five–compartment social–demographic model reveals how interactions between the marriage class, long–distance partnerships, affairs, divorce processes, and the age–structured population jointly govern the long–term behaviour of the system. The positivity and boundedness results guarantee that, for nonnegative initial data and biologically meaningful parameters, all solution trajectories remain within a well–defined positively invariant region. This ensures that the model is mathematically well posed and that its equilibria are dynamically attainable. A complete classification of all equilibrium points was established, including trivial, boundary, and fully endemic equilibria. Two equilibria arise generically in nondegenerate parameter regimes: (i) the *age-only equilibrium*, in which all social compartments vanish and only the age–structured subsystem persists, and (ii) the *interior equilibrium*, which represents a persistent coexistence of all demographic states. Other apparent equilibria (e.g., no-affair or partial–population states) reduce algebraically to these two when model parameters satisfy their usual positivity conditions. Linearization around each equilibrium produces a Jacobian matrix with a block-triangular structure, enabling stability

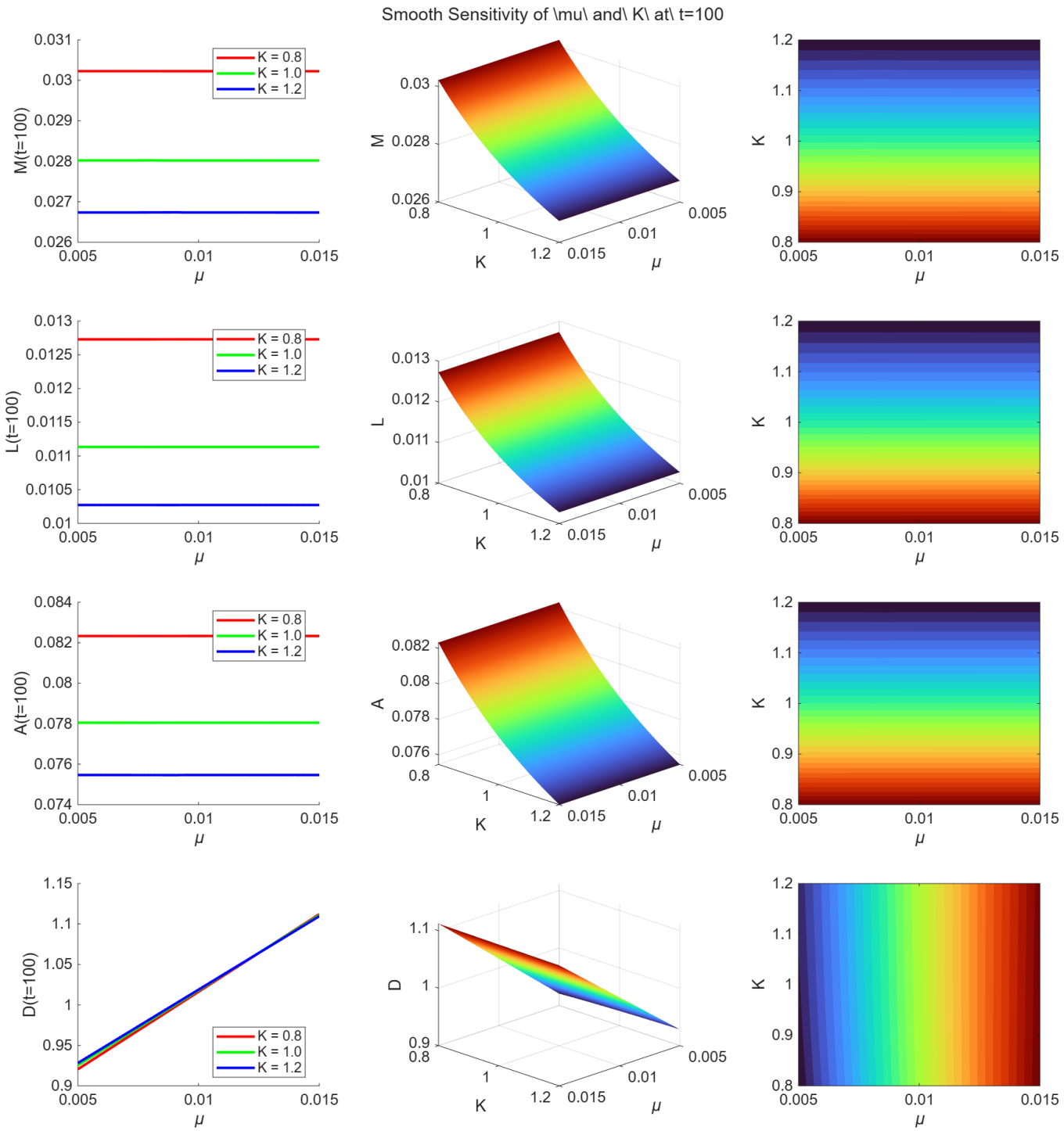

Figure 9. Sensitivity of the long-term compartment values with respect to the marriage dissolution rate μ and the affair-saturation threshold K at $t = 100$.

to be characterized by the spectrum of a reduced cubic polynomial. The Routh–Hurwitz conditions provide explicit inequalities on the model parameters that determine whether small disturbances decay or amplify. Stability requires all coefficients of the cubic to be positive and to satisfy the nonlinear inequality $c_1c_2 > c_3$; this inequality plays the role of a threshold separating stable and unstable parameter regimes. The age–structured modes remain stable whenever the natural departure rate $\mu_u(a)$ is positive, so instability can only arise through the social interaction parameters. The analytical results are supported by numerical stability regions computed across a broad range of parameter values. These simulations illustrate that destabilisation occurs primarily when the transition rates associated with marital breakdown and extramarital involvement (notably α_1, α_2, and β) become sufficiently large

relative to stabilising transitions such as reconciliation, distance separation, or dissolution rates (λ, δ, and γ). The resulting stability landscapes consistently show that the equilibrium loses stability once the combined social reinforcement mechanisms exceed the balancing demographic effects.

In summary, the model highlights how the interplay between social transitions and age–structured dynamics governs long-term outcomes. The Routh–Hurwitz threshold provides an analytically precise stability boundary, while the numerical parameter scans demonstrate the regions in which persistent fluctuations or runaway social changes may occur. Together, these results contribute to a deeper theoretical understanding of how demographic and behavioural processes interact to shape the evolution of complex social structures.

Data Availability Statement

Data will be made available on request.

Funding

This work was supported without any funding.

Conflicts of Interest

The authors declare no conflicts of interest.

Ethical Approval and Consent to Participate

Not applicable.

References

[1] Tessema, H., Haruna, I., Osman, S., & Kassa, E. (2022). A mathematical model analysis of marriage divorce. *Communications in Mathematical Biology and Neuroscience, 2022*, 15. [CrossRef]

[2] Mikolai, J., & Kulu, H. (2018). Short- and long-term effects of divorce and separation on housing tenure in England and Wales. *Population Studies, 72*(1), 17–39. [CrossRef]

[3] Duato, R., & Jódar, L. (2013). Mathematical modeling of the spread of divorce in Spain. *Mathematical and Computer Modelling, 57*(7-8), 1732-1737. [CrossRef]

[4] Olaniyi, A. A. (2015). Analytical study of the causal factors of divorce in African homes. *Research on humanities and social sciences, 5*(14), 18-29.

[5] Clark, S., & Brauner-Otto, S. (2015). Divorce in sub-Saharan Africa: Are unions becoming less stable? *Population and Development Review, 41*(4), 583–605. [CrossRef]

[6] Kleinsorge, C., & Covitz, L. M. (2012). Impact of divorce on children: Developmental considerations. *Pediatrics in Review, 33*(4), 147–155. [CrossRef]

[7] Fagan, P. F., & Churchill, A. (2012). The effects of divorce on children. *Marri Research, 1*(1), 1-48.

[8] Gambrah, P. P., & Adzadu, Y. (2018). Mathematical model of divorce epidemic in Ghana. *International Journal of Statistics and Applied Mathematics, 3*(2), 395-401.

[9] Diekmann, O., Heesterbeek, J. A. P., & Metz, J. A. J. (1990). On the definition and the computation of the basic reproduction ratio R 0 in models for infectious diseases in heterogeneous populations. *Journal of mathematical biology, 28*(4), 365-382. [CrossRef]

[10] Van den Driessche, P., & Watmough, J. (2002). Reproduction numbers and sub-threshold endemic equilibria for compartmental models of disease transmission. *Mathematical biosciences, 180*(1-2), 29-48. [CrossRef]

[11] Heffernan, J. M., Smith, R. J., & Wahl, L. M. (2005). Perspectives on the basic reproductive ratio. *Journal of the Royal Society Interface, 2*(4), 281-293. [CrossRef]

Dr. Sarita Pippal is an Assistant Professor in the Department of Mathematics, Panjab University, Chandigarh, India. She has been serving in this position since 2014, following her tenure at Ramjas College, University of Delhi. Her research interests include heat and mass transfer, fluid dynamics, fractional calculus, and mathematical modelling of natural and mixed convection flows. Dr. Pippal has published several research papers in reputed international journals and has presented her work at national and international conferences. She has also delivered invited talks, supervised doctoral research, and participated in various faculty development programs and workshops. Beyond academics, she enjoys dancing, cycling, and reading. (Email: saritamath@pu.ac.in)

Prof. (Dr.) Ajay Ranga is a Professor of Law at the University Institute of Legal Studies, Panjab University, Chandigarh. Presently, he is serving as Registrar, J. C. Bose University of Science and Technology, YMCA, Faridabad (Haryana). He has been the Professor of Law and served as Registrar (Off.), Finance Officer (Off.), and Director, Centre for Criminology and Forensic Science at Himachal Pradesh National Law University, Shimla. His academic qualifications include B.A. (Law), LL.B., LL.M., UGC-NET, and Ph.D. He has been a Fellow (Senator) of Panjab University and a member of its Executive Council, Academic Council, and Finance Committee.
He has served on numerous committees related to admissions, scholarships, faculty selection, curriculum development, and governance reforms. Prof. Ranga has also been part of several inspection committees of the Bar Council of India for evaluating law colleges across India. Additionally, he has been an observer for various government recruitment examinations and university entrance tests. A number of research scholars have completed LL.M. and Ph.D. research work under his guidance. He has delivered invited lectures on Constitutional Law, Governance, the Right to Information, Forensic Science, and Jurisprudence. (Email: ajayranga@pu.ac.in)